

Analog Integrated Circuits

ANALYSIS AND DESIGN OF A DOUBLE  
BALANCED GILBERT CELL BASED  
MIXER IN AMI06 TECHNOLOGY

Enrico Maria Renzi  
Roberto Rubino

June 17, 2018



## Contents

|          |   |           |
|----------|---|-----------|
| <b>1</b> | <b>Introduction</b>                                     | <b>1</b>  |
| 1.1      | A brief glimpse on mixers . . . . .                     | 1         |
| 1.2      | Figures of merit . . . . .                              | 3         |
| <b>2</b> | <b>Analysis of a Gilbert cell based multiplier</b>      | <b>7</b>  |
| 2.1      | Gilbert cell overview . . . . .                         | 7         |
| 2.2      | Gilbert cell circuit analysis . . . . .                 | 8         |
| 2.3      | Mathematical analysis: conversion gain . . . . .        | 14        |
| <b>3</b> | <b>Design by hand of a down-converting Gilbert cell</b> | <b>19</b> |
| 3.1      | Design specifications . . . . .                         | 19        |
| 3.2      | Gilbert cell design flow . . . . .                      | 20        |
| <b>4</b> | <b>Design by simulation</b>                             | <b>25</b> |
| 4.1      | Gilbert Cell design . . . . .                           | 25        |
| 4.2      | Biasing network design . . . . .                        | 30        |
| 4.3      | Validating design of the bias point . . . . .           | 34        |
| <b>5</b> | <b>Layout of the Gilbert Cell</b>                       | <b>37</b> |
| 5.1      | Differential RF stage . . . . .                         | 37        |
| 5.2      | Differential LO stages . . . . .                        | 39        |
| 5.3      | Current mirror and diode connected transistor . . . . . | 39        |
| 5.4      | Capacitors . . . . .                                    | 41        |
| 5.5      | Resistors . . . . .                                     | 44        |
| 5.6      | Putting together the layout . . . . .                   | 46        |
| <b>6</b> | <b>Simulation vs schematic comparison</b>               | <b>49</b> |
| 6.1      | Simulation setup . . . . .                              | 49        |
| 6.2      | Bandwidth evaluation . . . . .                          | 51        |
| 6.3      | Maximum conversion gain vs LO . . . . .                 | 53        |
| 6.4      | Time domain mixed signal . . . . .                      | 55        |
| 6.5      | Conversion gain and 1dB compression point . . . . .     | 55        |
| 6.6      | Single tone third order distortion . . . . .            | 57        |
| 6.7      | Two tone $IM_3$ and $CIM_3$ ratio . . . . .             | 60        |
| <b>7</b> | <b>Conclusions</b>                                      | <b>65</b> |



There are many deadlocks and dependencies which have to be taken into consideration [...] in order to satisfy the above design constraints. All the calculated values are changed based on the parametric analysis of transistors in Cadence Virtuoso.

II.4. The necessity of making a major design change increases as the fabrication of the system approaches completion.

III.3 All constants are variables.

*(Murphy's corollaries to the discipline of electronics engineering)*



# 1 Introduction

## 1.1 A brief glimpse on mixers

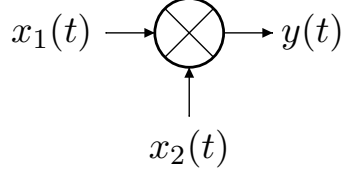


**Figure 1:** Representation of a mixer

An analog multiplier, also known as mixer, is a circuit that performs the product between two signals. As we will see, this feature can be exploited to convert informations from a certain frequency band to another by means of the intrinsic non-linear behaviour of this net. Supposing to have two sinusoidal signals

$$\begin{aligned}x_1(t) &= A_1 \cos(\omega_1 t + \varphi_1) \\x_2(t) &= A_2 \cos(\omega_2 t + \varphi_2)\end{aligned}$$

and the ideal mixer shown in figure 1, the out-coming signal  $y(t)$  is given by:

$$\begin{aligned}y(t) &= x_1(t) \cdot x_2(t) \\&= A_1 A_2 \cos(\omega_1 t + \varphi_1) \cos(\omega_2 t + \varphi_2) \\&= \frac{A_1 A_2}{2} \{ \cos[(\omega_1 - \omega_2)t + \varphi_1 - \varphi_2] + \cos[(\omega_1 + \omega_2)t + \varphi_1 + \varphi_2] \} \\&= A \cos(\omega_{LF} t + \varphi_{LF}) + A \cos(\omega_{HF} t + \varphi_{HF})\end{aligned}$$

where

$$\begin{aligned}\omega_{LF} &= |\omega_1 - \omega_2| \\ \omega_{HF} &= |\omega_1 + \omega_2| \\ \varphi_{LF} &= \varphi_1 - \varphi_2 \\ \varphi_{HF} &= \varphi_1 + \varphi_2\end{aligned}$$

Therefore, it comes that two signals with different frequency allocation are obtained at the output port: the first one at  $\omega_{LF} < \omega_1, \omega_2$  will be the down-converted component whereas the second, with  $\omega_{HF} > \omega_1, \omega_2$ , will be the up-converted one. Moreover, it is possible to select only one of these two signals by properly filtering out the unwanted part. Overall one can read the process as a modulation of an input signal by means of a carrier. Since the mixer is a bidirectional three-port, one can distinguish:

- The high frequency signal, RF. In case of down-conversion this is one input of the circuit, vice-versa it is the output (after filtering).
- The intermediate frequency signal, IF. In case of up-conversion this is one input of the circuit, vice-versa it is the output (after filtering).
- The local oscillator, LO. This is the carrier and it is always an input with known frequency.

Based on the above, it turns out that to mix-up two signals a non-linear device is needed, since the input components are at different frequency with respect to the output and a non-linear relation between voltages and currents appears. In general, mixing can be carried out by time-varying systems that can be implemented using:

**passive devices:** typically switches (diodes and transistors). In this case the mixing process introduces a *loss* since the output power is always less than the input one.

**active devices:** amplifying devices are used in active region providing *gain*.<sup>1</sup> They are more power consuming and less noisy than passive mixers.

Another way to classify mixers is the following:

**Single balanced mixers:** One or both input signals can pass to output, but it is not possible to suppress both of them,

**Double balanced mixers:** Thanks to symmetry in the net both the input and the LO are rejected at the output port. They show better isolation between ports than SBM.

To understand why a transistor can be used, let's consider the non-linear quadratic model for a nMOSFET. Supposing to drive it by injecting a two tone signal  $v_{GS}(t) = v_{RF}(t) + v_{LO}(t)$  at the gate (down-conversion configuration). One has:

$$\begin{aligned} i_D(t) &= k(v_{GS}(t) - V_{th})^2 \\ &= k(v_{RF}(t) + v_{LO}(t) - V_{th})^2 \\ &= k[v_{RF}^2(t) + v_{LO}^2(t) + 2v_{RF}(t)v_{LO}(t) - 2(v_{RF}(t) + v_{LO}(t))V_{th} + V_{th}^2] \end{aligned}$$

Supposing now  $v_{RF} \ll v_{LO}$ :

$$\begin{aligned} i_D(t) &\simeq k(v_{LO}(t) - V_{th})^2 + 2k(v_{LO}(t) - V_{th})v_{RF}(t) \\ &= I_D(t) + g_m(t)v_{RF}(t) \end{aligned}$$

---

<sup>1</sup>The definition of the gain and loss in mixer is different with respect to the one of linear devices, and will be discussed further.



hence, the model becomes a *quasi-linear* time-varying *small signal model* and the device operates in the *Small Signal Large Signal* regime (SSLS), because we still have the product of the two input signals through the transconductance. It is worth it to notice that depending on the amplitude of the RF (the LO is always driven in large signal), mixing can be obtained both in linear region or through second order non-linearity (fully non-linear device). A more detailed analysis about how to drive a mixer follows in section 2.

## 1.2 Figures of merit

Similarly to linear circuits, even in case of mixers it is possible to define the concept of gain. Actually, gain is defined only in case of linear systems, but this figure of merit is necessary to qualify the performance of the conversion stage. In case of non-monochromatic signals (general case) one defines the *voltage conversion gain* as:

$$A_v = \frac{V_{IF,rms}}{V_{RF,rms}}$$

moreover, one has that the output power is proportional to LO power (that is also called a *pump*), even if this dependency does not appear explicitly.

An important figure of merit concerning mixers is given by the 1dB compression point of the  $P_{in}/P_{out}$  characteristic. By increasing the value of the RF signal, the amount of harmonics at the output besides the fundamental IF frequency increases as well, eventually saturating the output (gain compression or flatness). This is due to the fact that power is no more mainly carried by the fundamental output tone (i.e. the IF tone), but it is rather shared by all the growing up harmonics. In other words the conversion gain stops to be constant, reduces itself, and the output waveform is clipped. Supposing to have input and output impedance matching one has that:

$$\begin{aligned} A_{conv} &= \frac{P_{IF}}{P_{RF}} \\ 10 \log_{10} A_{conv} &= 10 \log_{10} \frac{P_{IF}}{P_{RF}} \\ 10 \log_{10} P_{IF} &= 10 \log_{10} A_{conv} + 10 \log_{10} P_{RF} \\ P_{IF}|_{dB_m} &= A_{conv}|_{dB} + P_{RF}|_{dB_m} + 30dB \end{aligned}$$

This suggests both that the ideal output characteristic looks linear in logarithmic scale until the gain does not compress. The 1dB compression point can be defined as the input RF power at which:

$$P_{IF}|_{-1dB} = A_{conv}|_{dB} + P_{RF}|_{dB} - 1dB$$

hence:

$$P_{IF}|_{-1dB} = P_{IF}|_{dB,ideal} - 1dB$$

Other important figures of merit concern the third order distortions, that can be defined as follow:

**Third Order Distortion** In this case the input is a monochromatic signal. Because of the intrinsic device's non-linearity, the output signal contains frequency components not present at the input. It can be demonstrated that the most important spurious contribution on output fundamental tone comes from the third order term, in fact, by expanding the device's output current in Taylor's series and supposing a monochromatic gate signal, one has:

$$\begin{aligned} i_D(t) &= I_D|_{V_{GS}} + av_{gs}(t) + bv_{gs}^2(t) + cv_{gs}^3(t) + \dots \\ &= I_D|_{V_{GS}} + i_{D,fund}(t) + i_{D,SOD}(t) + i_{D,TOD}(t) + \dots \end{aligned} \quad (1)$$

Where  $a > b > c$ . Developing the first three terms of the series expansion one has:

$$i_{D,fund}(t) \propto a \cos(\omega_0 t) \quad (2)$$

$$i_{D,SOD}(t) \propto b \cos^2(\omega_0 t) = \frac{1}{2}b + \frac{1}{2}b \cos(2\omega_0 t) \quad (3)$$

$$i_{D,TOD}(t) \propto c \cos^3(\omega_0 t) = \frac{3}{4}c \cos(\omega_0 t) + \frac{1}{4}c \cos(3\omega_0 t) \quad (4)$$

It is straightforward that the third order term yields an additive contribution exactly at the fundamental tone, whereas the second order distortion adds a zero-frequency term that is not interfering with in-band signal (a balanced configuration can reject DC component). In general, even order distortions (2<sup>nd</sup>, 4<sup>th</sup> ...) contributes in corrupting the output signal as well, though they are less important. Also 5<sup>th</sup> order distortion exist, for which the same reasoning holds. All harmonic components introduced by input stage are moved in frequency by mixing stages and can cause in-band spurious components.

**Third Order Intermodulation, IM<sub>3</sub>** This distortion comes from a two-tone input injection ( $f_1 = f_0$  and  $f_2 = f_0 + \delta f$ ). Due to intermodulation between tones, unwanted frequencies are generated. The most important contribution comes from the third order intermodulation (IM3):  $|m| + |n| = 3$  and  $m \cdot n < 0$  (where  $m = \pm 2, \pm 1$  and  $n = \pm 2, \pm 1$  are the intermodulation indexes). Taking  $m = 2$  and  $n = -1$ :

$$f_{IM3}|_{\substack{m=2 \\ n=-1}} = 2f_1 - f_2 = f_0 - \delta f$$

that is clearly an in-band distortion. It can be demonstrated that, in case of same input and output reference impedance, the out and in

intermodulation points are related to stage's gain and first harmonics's output power:

$$\begin{aligned} OIP_3|_{dB} &= \frac{3}{2}P_{out,1st}|_{dB} - \frac{1}{2}P_{out,IM3}|_{dB} \\ IIP_3|_{dB} &= OIP_3|_{dB} - A_{v,1st}|_{dB} \end{aligned}$$

By taking  $m = -1$  and  $n = 2$  one has instead:

$$f_{IM3}|_{\substack{m=2 \\ n=1}} = -f_1 + 2f_2 = f_0 + \delta f$$

We notice that the whole spectrum presents side-bands produced by intermodulation. This phenomenon is called *spectral regrowth* and it can be quantified by the *Carrier to Intermodulation Ratio (CIM)*. In case of mixing we change frequency band from input to output, anyway the previous result holds:

$$f_{IF,IM3}|_{\substack{m=2 \\ n=1}} = 2f_{RF1} - f_{RF2} - f_{LO} = f_{IF} - \delta f$$



## 2 Analysis of a Gilbert cell based multiplier

### 2.1 Gilbert cell overview

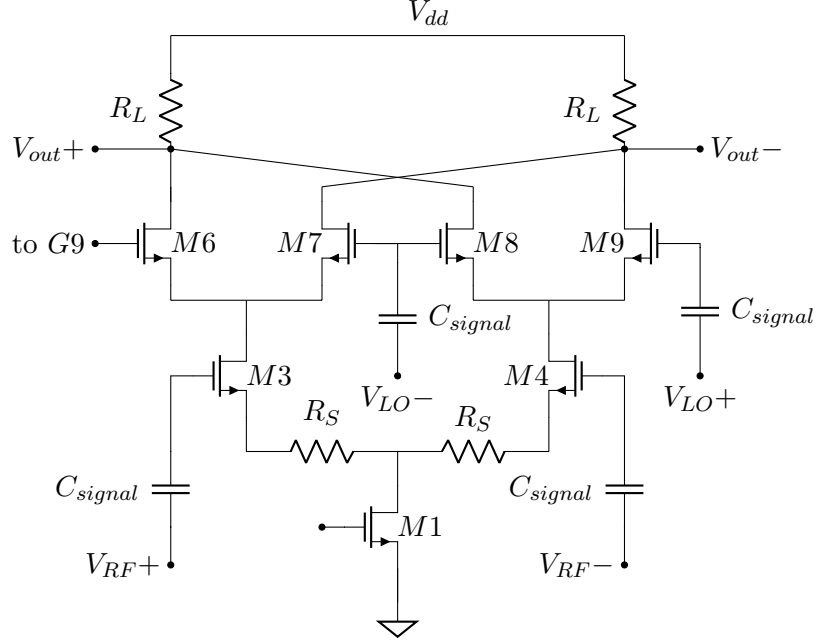


**Figure 2:** Gilbert cell mixer

A possible implementation of a CMOS Gilbert cell based mixer is shown in figure 2, whereas the biasing network can be found in figure 3. This circuit exploits a differential topology to implement a double-balanced cell, providing:

- Reasonable conversion gain (from one to some tens);
- Good input frequencies rejection at the output port, along with high linearity, thanks to the double-balanced topology;<sup>2</sup>
- Good isolation between ports is provided by the strong suppression of spurious frequency components;

<sup>2</sup>The linearity is meant with respect to the conversion gain.

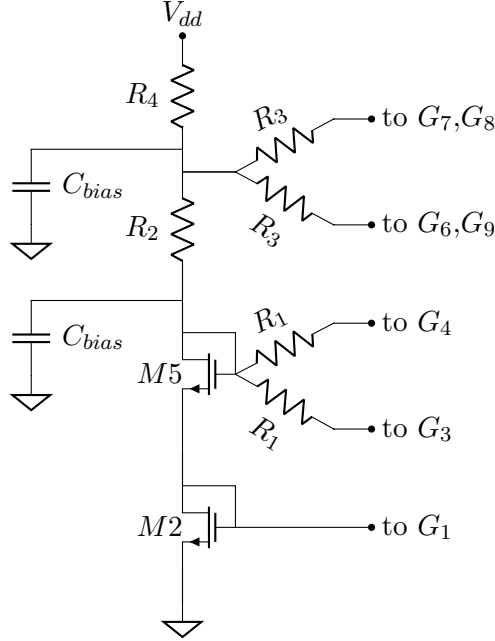


**Figure 3:** Biasing network

## 2.2 Gilbert cell circuit analysis

To analyse the circuit it is necessary to give some information about the topology, how it is biased and driven. Looking at figures 2 and 3 it is possible to identify five main blocks that are described hereafter.

**Bias net** This net is made up of a current mirror (transistors M1 and M2, figure 4) and the voltage reference generation network (transistor M5, R1, R2, R3, R4, R5, see figure 3).

Transistor M1 of the current mirror acts as a current sink for the differential pair made up by M3 and M4, fixing the biasing current for the whole circuit. M2 sinks the current of the bias net instead. Transistors which compose the current mirror's strong branch are biased in the saturation region, so that their high drain impedance approximates well the behaviour of a current sink. Being  $V_{G1} = V_{GS1}$  the gate voltage of M1 we have that the transistor works in saturation if:

$$V_{GS} \geq V_{th} \quad (5)$$

$$V_{DS} > V_{od} = V_{GS} - V_{th} \quad (6)$$

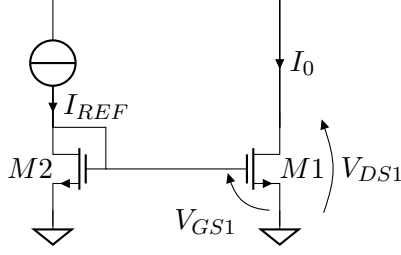


**Figure 4:** Current mirror

The same holds for M2, which is always in saturation condition since it is diode connected (provided 5). In saturation (neglecting channel modulation effects), one has that drain current only depends on the gate voltage and its expression is given by:

$$I_D = \mu_{n,eff} \frac{C_{ox}}{2} \frac{W}{L} (V_{GS} - V_{th})^2 = \frac{\beta_n}{2} V_{od}^2 \quad (7)$$

hence M1 stays in saturation till when:

$$V_{DS1} \geq V_{od1} = V_{th} - \sqrt{\frac{2I_0}{\beta_n}} \quad (8)$$

therefore to have a smaller value of overdrive voltage one should have larger transistors, i.e. large W. The output impedance is instead defined by:

$$r_o = \frac{1}{\lambda I_0} \propto L \quad (9)$$

where  $\lambda$  models the channel modulation effect. It appears that longer transistors are needed to have better current sinks. By looking at figure 4, one finds (supposing both M2 and M1 in saturation, and  $V_{GS1} = V_{GS2} = V_{DS1} = V_{DS2}$ ) that:

$$\begin{aligned} I_0 &= \frac{\beta_{n1}}{2} (V_{GS1} - V_{th})^2 (1 + \lambda_1 V_{DS1}) \\ I_{REF} &= \frac{\beta_{n2}}{2} (V_{GS1} - V_{th})^2 (1 + \lambda_1 V_{GS1}) \end{aligned}$$

hence, supposing to have equal technology parameters:

$$\frac{I_0}{I_{REF}} = \frac{W_1/L_1}{W_2/L_2} \quad (10)$$

Ideally the current mirroring depends only on geometrical parameters, meaning that a very good dimension matching is required. Even if the two devices are very close to each other within the same chip, the possibility to have

variations depending on temperature exists, i.e.  $V_{th}$  and  $\mu_{n,eff}$ . Supposing to have equal devices with everything constant but:

$$\begin{aligned}K_{n1} &= K_n + \Delta K_n \\V_{th,1} &= V_{th} + \Delta V_{th}\end{aligned}$$

one eventually finds that:

$$\frac{I_0}{I_{REF}} \simeq 1 + \frac{\Delta K_n}{K_n} + 2 \frac{\Delta V_{th}}{V_{od}}$$

Then, some of the possible mismatch causes are:

- $K_n$ , that can vary a lot in case of wide circuits;
- $V_{od}$ , that is usually set low and varies with  $V_{th}$ , whose small variations can produce large differences in the two currents;
- difference between  $V_{DS1}$  and  $V_{DS2}$ .

Assuming as maximum variations:

$$\begin{aligned}\frac{\Delta K_n}{K_n} &= \pm 5\% \\ \frac{\Delta V_{th}}{V_{GS} - V_{th}} &= \pm 10\%\end{aligned}$$

one has:

$$\frac{I_0}{I_{REF}} = 1 \pm 15\%$$

This means that actual current mirrors' implementation requires advanced topologies. A cascaded voltage divider is connected as load for M2:

- M5 is diode connected and it is used to generate the correct gate bias voltage for the gain stage.
- A resistive voltage divider made up of R2 and R4 is used to bias the mixing stage.
- Resistors R1 and R3 are used to connect the bias net to the gain and mixing stages' gates. They also acts as high impedance for the RF and LO signals coming from outside the circuit and prevents them to be injected into the bias net.
- Capacitors C1 and C2 shunt possible non-DC disturbances coming from the Gilbert Cell, improving the bias isolation.



Noise issues will not be analysed within this treatise, even if it should be considered for a complete design. As a rule of thumb, larger gates and low overdrive voltages should be used to lower noise contribution. Using resistors as voltage references can be detrimental in case of supply fluctuations, since a resistive divider cannot reject them. However, using active devices, we would produce much more low frequency noise injection within the net (flicker noise).

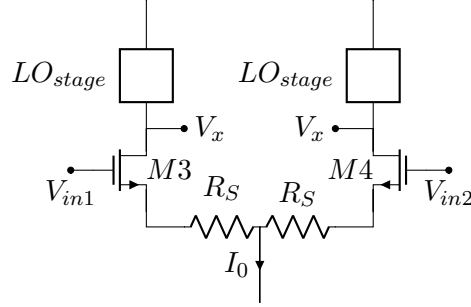


**Figure 5:** Gain stage.

**Gain stage** The gain stage (shown in figure 5) is the linear part of the mixer. It must handle the power coming from the input RF signal providing some amplification, introducing the smaller amount of distortion. The topology is a differential stage with source degeneration, well suited for linear application (thanks to the small amount of distortion). This stage is made up of two transistors (M3 and M4) in common source configuration, biased with current by M1, and two source degeneration resistances  $R_S$ .

The RF differential signal modulates the current flowing into each of the two transistors, that have to be biased in saturation region. For both of them it must be ensured a wide output voltage range and a quite small overdrive voltage, along with a large drain-to-source bias voltage (required to maintain the stage in saturation during the switching of the LO stage).

To have an idea about the gain that can be obtained with this stage, one can look at the one in figure 5. Removing degeneration resistances one finds that the gate-to-gate mesh gives:

$$V_{in,1} - V_{in,2} = V_{GS3} - V_{GS4}$$

from equation 7, recalling that  $I_1 + I_2 = I_0$  and squaring:

$$(V_{in,1} - V_{in,2})^2 = \frac{2}{\beta_n} (I_0 - 2\sqrt{I_1 I_2})$$

that once inverted yields:

$$I_1 - I_2 = \sqrt{\beta_n I_0} \cdot (V_{in,1} - V_{in,2}) \cdot \sqrt{1 - \frac{\beta_n}{4I_0} (V_{in,1} - V_{in,2})^2}$$

Writing the previous equation in term of  $\Delta I = I_1 - I_2$  and  $\Delta V_{in} = V_{in,1} - V_{in,2}$  and computing the value of the slope of this characteristic, one obtains that the *maximum* differential voltage gain in equilibrium condition  $\Delta V_{in} = 0$  is given by:

$$|A_v| = \sqrt{\beta_n I_0} \cdot R_{L1} \quad (11)$$

This suggest that it is better to se the stage's bias exactly with  $V_{GS1} = V_{GS2}$ . A complete expression for equation 11 also gives that the differential transconductance is a strongly non-linear function of the gate bias voltage.

As we said before there it is the possibility to have mismatch between the transistors and the loads due to circuit dimensions, temperature distribution and process tolerances. Then, looking at figure 5,  $M3 \neq M4$  and  $R_1 \neq R_2$  (where input resistance of the LO stage). It can be demonstrated that the offset output voltage due to differences in the circuit parameters and dimensions is:

$$V_{o,offset} = \Delta V_{th} + \frac{V_{GS} - V_{th}}{2} \left( -\frac{\delta R}{2R} \frac{\Delta W/L}{2W/L} \right)$$

To reduce this error that would produce a wrong bias for the mixing stage a common centroid topology should be used in layout.

The small signal equivalent transconductance of the stage, once we added the source degeneration, is given by:

$$G_{m,eq} = \frac{g_m}{1 + g_m R_S} \quad (12)$$

By adding  $R_S$  we lower the RF stage's current gain, however we also get a more linear behaviour reducing its dependency with respect to the bias point (this fact will be demonstrated later).

The two transistors have their body contact connected to ground, this means that the threshold changes accordingly to the source to body voltage,  $V_{SB}$ :

$$V_{th} = V_{th0} + \gamma_B (\sqrt{2\phi_P + V_{SB}} - \sqrt{2\phi_P}) \quad (13)$$

This equation holds for all the transistors in the circuit, other than in current mirror.

**Mixing stage** This stage is also called *switching stage*, suggesting the way we want to drive transistors M6 to M9 (figure 6). Also this one has a differential topology, however, differently from RF stage, we drive each pair with complementary LO signals that turn on and off cycle-by-cycle one of the two devices. A sinusoidal signal is applied to the gates (similarly it can be used a square wave), large enough to ensure the abrupt switching of the stage: when a device is on, it must be in saturation (not in triode! These are actually *switch-like* transistors), while the other one must be completely interdicted.

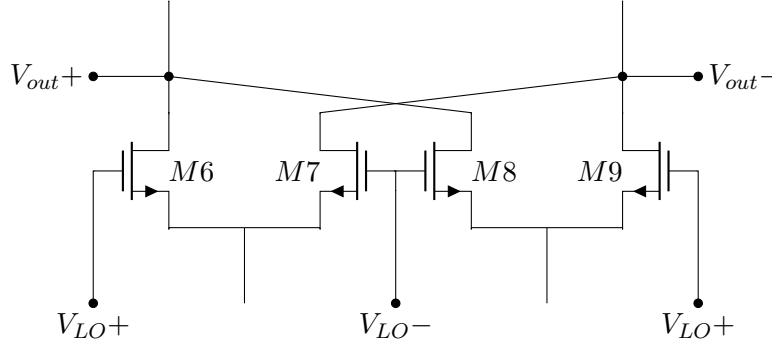


**Figure 6:** Mixing stage

A compromise is needed since:

- small amplitude of LO signals produce slower switching speed, hence part of the power is wasted as common mode signal at the output;
- too large LO signals drive the MOSFET in triode region producing spikes that corrupt the output signal with unwanted feed-through and reduces gain.

Switching speed is related to the device cut-off frequency, that for short channel devices is inversely proportional to channel length and linearly dependent to the overdrive voltage:

$$f_T \propto V_{od}/L$$

suggesting that the highest overdrive and the minimum channel length should be chosen. The maximum operating frequency should be at least ten times lower than  $f_T$ . Again, a compromise must be found among the following solutions:

- Setting the minimum available length (fixed by the design kit);
- Selecting higher overdrive voltage one has the possibility to increase  $f_T$ , however to keep our switches in saturation and to obtain a large output swing we need to keep small this quantity;
- Widening the gate width one has faster device, unfortunately the source to bulk capacitance would increase, eventually shunting the RF signal coming from the LNA stage to ground;
- Reducing the current a faster commutation is achieved, along with lower transconductance though.

Even if the switching stage is not linear it is possible to define its static gain analysing a single pair. Recalling that the gate LO signal modulates

the stage drain current as a square wave, that can be written in term of its Fourier's series:

$$i_D(t) = I_{pk} \left( \frac{1}{2} - \frac{2}{\pi} \sum_{n=1,3,5\dots} \frac{1}{n} \sin(n\omega t) \right)$$

where only odd harmonics are present. The instantaneous gain fo the stage, related to the first harmonic is:

$$A_c|_{switch} = \frac{2}{\pi} \quad (14)$$

that is neither dependent on the bias of the stage nor on the actual device transconductance.<sup>3</sup> It is important to notice that equation 14 is exact in case of gate's square wave signals, whereas in case of sinusoidal driving the actual gain will be reduced because of the smoother variation of the drain current waveform.

**Load stage** The load stage is formed by two resistors  $R_L$  whose role is to give the stage enough gain and to set the output bias voltage through the RF drain current. They must be as matched as possible to make the differential outputs of the Gilbert cell equals.

### 2.3 Mathematical analysis: conversion gain

As already stated a mixer is a non-linear time variant system, hence a descriptive approach based on the behaviour of the cell is well suited to find the conversion gain of the cell.<sup>4</sup> The following analysis is based on the schematic in figure 7.

We suppose all the transistors in the gain and bias stage working in saturation, then we identify:

- $i_3$  and  $i_4$  the current through M3 and M4;
- $i_6$  and  $i_7$  the current through M6 and M7;
- $i_8$  and  $i_9$  the current through M8 and M9;
- $i_{o1}$  the current through  $R_{L1}$ ;
- $i_{o2}$  the current through  $R_{L2}$ ;

---

<sup>3</sup>It is however important to remember what stated above, regarding the intensity of the applied gate voltage, that further reduces this quantity in case of too large input signals. Moreover its better to notice that the stage introduces a loss rather than an actual gain.

<sup>4</sup>It is not possible to use neither the superposition of effect nor the Laplace transform to compute the gain due to the presence of the switching pairs.

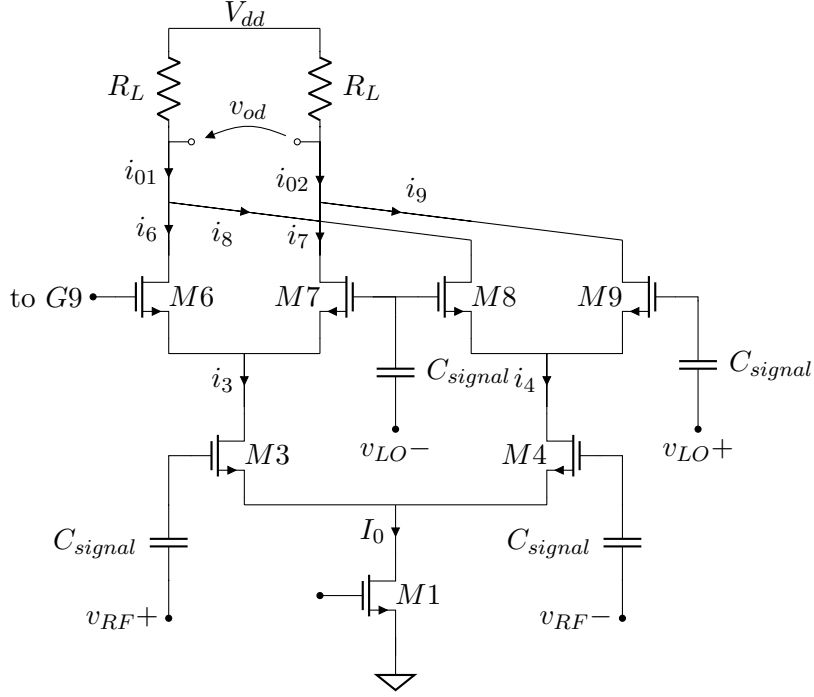


**Figure 7:** Gilbert cell, to be use as a reference for the mathematical analysis

- $I_D$  the bias current, equal to  $\frac{I_0}{2}$ ;
- $i_{od}$  the output differential bias current;
- $S(t) = \frac{1}{2} - \frac{2}{\pi} \sum_{n=1,3,5,\dots} \frac{1}{n} \sin(n\omega_{LO}t)$  is the switching function of the mixing cell (then we consider the LO stage as it was made up of ideal switches).

The differential input RF signal is given by:

$$v_{RF}(t) = \frac{V_{RF}}{2} \cos(\omega_{RF}t) \quad (15)$$

Currents flowing into the two RF stages are given by:

$$i_3(t) = I_D + i_d(t) \quad (16)$$

$$i_4(t) = I_D - i_d(t) \quad (17)$$

where, from equation 12, the  $i_d$  current is a small signal variation given by:

$$\begin{aligned} i_d(t) &= I_{RF} \cos(\omega_{RF}t) \\ &= G_{m3,4} \frac{V_{RF}}{2} \cos(\omega_{RF}t) \end{aligned} \quad (18)$$

It is now possible to define the current flowing into the switching stage recalling that they are discontinuous functions modulated by the switching function  $S(t)$ :

$$i_6(t) = [I_D + i_d(t)]S(t) \quad (19)$$

$$i_7(t) = [I_D + i_d(t)]S(t - T_{LO}/2) \quad (20)$$

and

$$i_8(t) = [I_D - i_d(t)]S(t - T_{LO}/2) \quad (21)$$

$$i_9(t) = [I_D - i_d(t)]S(t) \quad (22)$$

because M6 and M9 share the same LO signal; the same holds for M7 and M8. Hence the current through  $R_{L1}$  and  $R_{L2}$  is given by:

$$\begin{aligned} i_{o1}(t) &= I_6(t) + I_8(t) \\ &= [I_D + i_d(t)]S(t) + [I_D - i_d(t)]S(t - T_{LO}/2) \end{aligned} \quad (23)$$

and

$$\begin{aligned} i_{o2}(t) &= I_7(t) + I_9(t) \\ &= [I_D + i_d(t)]S(t - T_{LO}/2) + [I_D - i_d(t)]S(t) \end{aligned} \quad (24)$$

Therefore, the output differential current is:

$$\begin{aligned} i_{od}(t) &= i_{o1}(t) - i_{o2}(t) \\ &= 2i_d(t)S(t) - 2i_d(t)S(t - T_{LO}/2) \end{aligned} \quad (25)$$

Noticing that:

$$\begin{aligned} S(t - T_{LO}/2) &= \frac{1}{2} - \frac{2}{\pi} \sum_{n=1,3,5,\dots} \frac{1}{n} \sin(n\omega_{LO}t - T_{LO}/2) \\ &= \frac{1}{2} + \frac{2}{\pi} \sum_{n=1,3,5,\dots} \frac{1}{n} \sin(n\omega_{LO}t) \\ &= 1 - \frac{1}{2} + \frac{2}{\pi} \sum_{n=1,3,5,\dots} \frac{1}{n} \sin(n\omega_{LO}t) \\ &= 1 - S(t) \end{aligned} \quad (26)$$

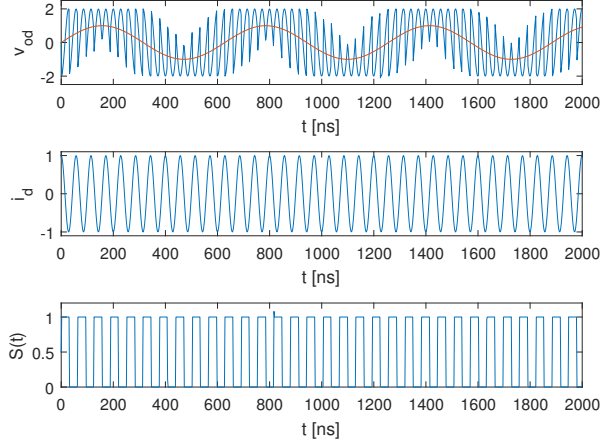


**Figure 8:** Ideal signal modulation within Gilbert cell.

and substituting equation 26 in 25 we get:<sup>5</sup>

$$\begin{aligned}
 i_{od}(t) &= -\frac{8i_d(t)}{\pi} \sum_{n=1,3,5\dots} \frac{1}{n} \sin(n\omega_{LO}t) \\
 &= -\frac{8I_{RF}}{\pi} \cos(\omega_{RF}t) \sum_{n=1,3,5\dots} \frac{1}{n} \sin(n\omega_{LO}t) \\
 &= -\frac{8I_{RF}}{\pi} \sum_{n=1,3,5\dots} \frac{1}{n} \cos(\omega_{RF}t) \sin(n\omega_{LO}t) \\
 &= -\frac{8I_{RF}}{\pi} \sum_{n=1,3,5\dots} \frac{1}{2n} \left\{ \sin[(\omega_{RF} + n\omega_{LO})t] + \sin[(\omega_{RF} - n\omega_{LO})t] \right\}
 \end{aligned} \tag{27}$$

The full ideal output differential signal is shown in figure 8. Considering only the fundamental tone of the LO signal (other frequency terms are out-of-band with respect to IF) and multiplying by  $R_L = R_{L1} = R_{L2}$  one finds that the differential output voltage is given by:

$$\begin{aligned}
 v_{od}(t) &= -\frac{4I_{RF}R_L}{\pi} \{ \sin[(\omega_{RF} + \omega_{LO})t] + \sin[(\omega_{RF} - \omega_{LO})t] \} \\
 &= -\frac{4I_{RF}R_L}{\pi} [\sin(\omega_{HF}t) + \sin(\omega_{IF}t)]
 \end{aligned} \tag{28}$$

then, referring to the IF component:

$$\begin{aligned}
 v_{od,IF}(t) &= -\frac{4I_{RF}R_L}{\pi} \sin(\omega_{IF}t) \\
 &= -\frac{2G_{m3,4}R_LV_{RF}}{\pi} \sin(\omega_{IF}t)
 \end{aligned} \tag{29}$$

---

<sup>5</sup>  $\cos(x)\sin(y) = \frac{1}{2}\sin(x+y) + \frac{1}{2}\sin(x-y)$

that, considering the IF and RF *rms* values eventually yields the Gilbert cell mixer conversion gain:

$$A_{vC} = \frac{2}{\pi} \frac{R_L}{\frac{1}{g_{m3,4}} + R_S} \quad (30)$$

Notice that the very same expression could have been derived in a faster way by inspection, multiplying LO's conversion gain by RF equivalent transconductance. This is possible only since LO's gain is independent on  $V_{LO}$ , therefore the operation can be treated as linear. Namely:

$$\begin{aligned} A_{vC} &= \frac{2}{\pi} \frac{g_{m3,4}}{1 + g_{m3,4}R_S} R_L \\ &= \frac{2}{\pi} G_m R_L \end{aligned} \quad (31)$$

It is now possible to highlight that:

- in first approximation the conversion gain does not depends on the amplitude of the LO signal;
- both LO and RF components are rejected at the output;
- it is possible to keep only the IF component by filter out the HF signal;
- the degeneration resistance  $R_S$  improve the stage's linearity. In fact, if properly chosen, one has:  $A_{vC}|_{g_{m3,4} \ll R_S} \simeq \frac{2}{\pi} \frac{R_L}{R_S}$ . Besides to linearity, the conversion gain is less sensitive with respect to the RF stage bias point;
- no informations about frequency behaviour appear with this kind of analysis.



### 3 Design by hand of a down-converting Gilbert cell

#### 3.1 Design specifications

The design specifications follow:

- The use technology is the MOSIS AMI  $0.6\mu\text{m}$ . **Loose constraints regarding maximum gate width have been considered. This technology is nowadays old-fashioned, hence this project has only didactic purposes.** Cadence Design Environment has been used to carry on the project;
- the supply voltage is  $V_{DD}=5\text{V}$ ;
- the design is about a down-conversion mixer. The analysis will be carried on considering two monochromatic signals  $f_{RF}=110\text{ MHz}$  and  $f_{LO}=100\text{ MHz}$ , producing a wanted baseband signal at  $f_{IF}=10\text{ MHz}$  (the HF component is considered as filtered out);
- all the transistors should work in saturation;
- the conversion gain is chosen accordingly to the previous specification equal to  $A_{vC}=4$ .

The most important parameters used in the design are reported in the following table: <sup>6</sup>

**Table 1**

| Parameter  | Name                             | Value | Unit                      |
|------------|----------------------------------|-------|---------------------------|
| $A_{vC}$   | Voltage Conversion gain          | 5.6   |                           |
| $V_{DD}$   | Supply voltage                   | 5     | V                         |
| $I_0$      | Cell biasing current             | 5     | mA                        |
| $V_{th0}$  | n-MOS threshold w.o. body effect | 0.709 | V                         |
| $K_n$      | n-MOS physical parameter         | 116   | $\mu\text{A}/\text{V}^2$  |
| $I_{dss}$  | Maximum channel current density  | 466   | $\mu\text{A}/\mu\text{m}$ |
| $\phi_P$   | Fermi potential                  | 0.7   | V                         |
| $\gamma_B$ | Body effect coefficient          | 0.5   | V                         |
| $L_{min}$  | Technology minimum length        | 0.6   | $\mu\text{m}$             |

It is necessary to notice that the following calculation is carried on considering the easiest model among the physic-based models for a MOSFET, i.e. the level 1 model. Its aim is to make easy the understanding of design

<sup>6</sup>MOSFET's parameters are intended at  $T=27^\circ\text{C}$

choices which follow in next section. The final design rose the need to rely on the more complex model of the simulator which takes into account all sub-micron device non idealities such as the carrier velocity saturation and pronounced body effect.

### 3.2 Gilbert cell design flow

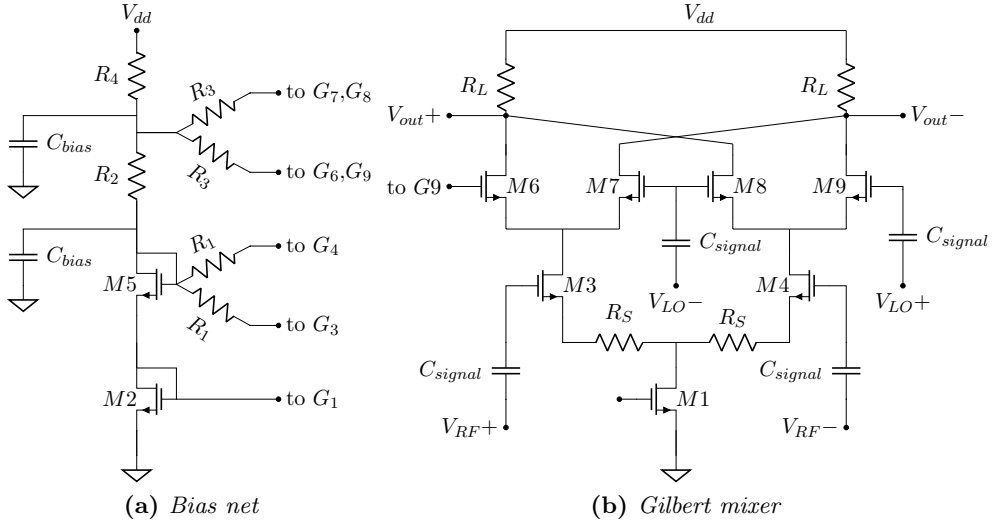


**Figure 9:** Bias net and Gilbert Mixer schematic

**Current mirror bias** Design has been developed on the schematic visible in figure 9. Both M1 and M2 must be in saturation. We choose the same current to flow in the weak and strong branches in order to have equal structures (this aids the circuit symmetry and matching, allowing us to use interdigitated structure). We impose:

$$I_{D1} = I_{D2} = I_0 = 5mA \quad (32)$$

$$V_{od1} = V_{od2} = 0.4V \quad (33)$$

$$L_1 = 3L_{mim} = 1.8\mu m \quad (34)$$

The current magnitude is chosen thinking about the mixer used in a transmitter receiving chain, after an hypothetical power stage. The overdrive voltage's value is chosen in order to keep turned on the stage even with fluctuations of the drain node. However, to have the same mirrored current

we must have:

$$\begin{aligned} V_{GS1} &= V_{GS2} \\ V_{DS1} &= V_{DS2} \\ \left(\frac{W}{L}\right)_1 &= \left(\frac{W}{L}\right)_2 \end{aligned}$$

suggesting that this kind of current source can work properly only with small signal variation coming from the RF stage. Now, by using 7, neglecting channel modulation effects and inverting:

$$W_1 = \frac{2I_0}{K_n V_{od1}^2} L_1 = 969.8 \mu m \quad (35)$$

Both M1 and M2 are not affected by body effect, then:

$$V_{th1} = V_{th2} = V_{th0}$$

hence:

$$V_{GS2} = V_{DS2} = V_{th0} + \sqrt{\frac{2I_0 L_1}{K_n W_1}} = 1.1V \quad (36)$$

The design for the voltage reference bias net is reported in section 4.

**Load stage and gain choice** As previously stated we chose  $A_{vC}=4$ . Since the whole differential structure must be symmetrical, current  $I_0$  is evenly split into M3 and M4: this is the same current flowing also into the two loads. In order to give the LO stage **enough output swing** we impose one third of the supply voltage must drop on the load. Therefore, we can evaluate the load resistance's value:

$$R_L = \frac{\frac{1}{3}V_{DD}}{I_0/2} = 667\Omega \quad (37)$$

**Gain stage bias** The design of the RF bias begins with the choice of its transconductance, fixed by  $A_{vC}$ ,  $R_L$  and  $R_S$ . We consider M3 and M4 equal and in saturation. The gate length for this stage is set

$$L_3 = L_4 = 3L_{min} = 1.8\mu m \quad (38)$$

The degeneration resistance's value is chosen in order to increase stage linearity without provoking a too large voltage drop on it. Given  $R_S$  equal to  $10\Omega$ :

$$V_{R_S} = \frac{R_S}{I_0/2} = 25mV \quad (39)$$

Now, by inverting equation 30:

$$g_{m3} = \frac{\pi}{2} \frac{1}{\frac{R_L}{A_{vC}} - R_S} = 10mS \quad (40)$$

We noticed that there are many variables involved which directly affect design feasibility:

- high values of  $R_S$  decrease the RF stage transconductance, requiring large transistors with low overdrives, but increase linearity. Low values lead instead to higher transconductance reducing the output dynamic though;
- increasing the conversion gain we have the same drawbacks of large transistors. Mixing signals is a strongly inefficient operation though, then conversion gain cannot be reduced too much;
- the choice of load is important to fix the output dynamic and must be done carefully.

By inverting equation 11:

$$W_3 = g_{m3}^2 \frac{2L_3}{K_n I_0} = 623.4 \mu m \quad (41)$$

We have body effect due to the source to body voltage, shared by M3 and M4:

$$V_{SB3} = V_{DS1} + V_{R_S} \quad (42)$$

then, from equation 13 we found an increased threshold voltage:

$$V_{th3} = V_{th0} + \gamma_B (\sqrt{2\phi_P + V_{SB3}} - \sqrt{2\phi_P}) = 0.957V \quad (43)$$

from which it comes that:

$$V_{od3} = \sqrt{\frac{I_0}{K_n W_3 / L_3}} = 0.353V \quad (44)$$

$$V_{GS3} = V_{th3} + V_{od3} = 1.731V \quad (45)$$

Unfortunately the value of the overdrive voltage looks quite large, requiring us to fix  $V_{DS3,4}$  high enough to avoid the stage to be turned off by LO's stage swing. We impose to have half the supply voltage to drop on the gain stage and current mirror, having (neglecting  $25mV$  drop on  $R_S$ ):

$$V_{DS3} = \frac{1}{2} V_{DD} - V_{DS1} = 1.4V \quad (46)$$

To ensure conduction of M3 and M2 we set:

$$V_{G3} = V_{GS3} + V_{R_S} + V_{DS1} = 2.805V \quad (47)$$

**Mixing stage bias** Also in this case we require transistors from M6 to M9 to be in saturation (they are equal and biased the same way). We reduce as much as possible the overdrive voltage: in this way the stage is kept nearby the threshold fostering a fast commutation of the switches. Having small overdrives produces large transistors then, to limit this we set LO transistor length to the minimum one:

$$L_6 = L_{min} \quad (48)$$

$$V_{od6} = 150mV \quad (49)$$

By using 7, taking in count the body effect and the fact that in each LO transistor flows half of the bias current when turned on, we get:

$$W_6 = 1.1mm \quad (50)$$

$$V_{SB6} = V_{DS1} + V_{R_S} + V_{DS3} \quad (51)$$

$$V_{th6} = 1.18V \quad (52)$$

This result does not consider short channel effects, that produce a more complex threshold dependency on source-bulk voltage. However, considering the simplest body effect model we have that the M6 to M9's bias gate voltage is:

$$V_{GS6} = 1.326V \quad (53)$$

$$V_{G6} = V_{GS6} + V_{DS1} + V_{R_S} + V_{DS3} = 3.855V \quad (54)$$



## 4 Design by simulation

### 4.1 Gilbert Cell design

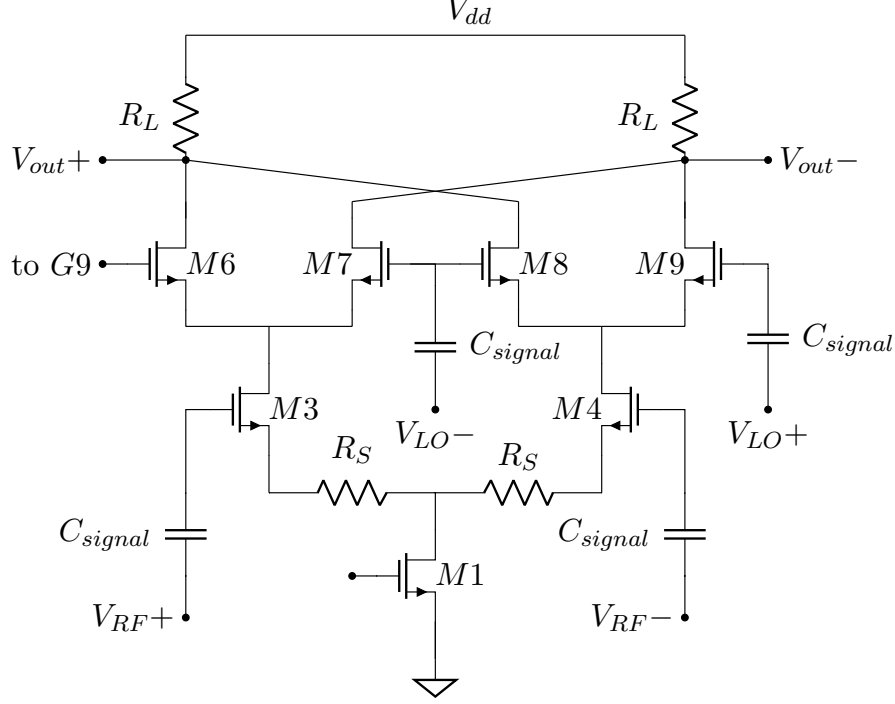


**Figure 10:** Reference schematic for the design of Gilbert mixer

After simulating the design made with Level 1 model, simulation results proven to be not enough accurate to have a correctly behaving circuit. For this reason a new design was carried on taking advantage of the simulated trans-characteristic of each stage.

In literature an optimum value for RF transistors width in mixers is proposed:<sup>7</sup>

$$W_{opt} = \frac{1}{3\omega LC_{ox}R_g} \quad (55)$$

where  $\omega$  is the stage's working frequency (i.e.  $f_{RF}$ ),  $L$  is the channel length,  $C_{ox}$  is the MOSFETS's total oxide capacitance and  $R_g$  the generator output resistance (we set this value equal to  $50\Omega$ ). Values coming from this formula are actually too large ( $\geq 1\text{mm}$ ), therefore we chose to pursue another approach to begin the design. The reference schematic is the one in figure 10.

<sup>7</sup>More generally, this gives a compromise between power dissipation and noise in LNA.

The starting specification was to maximize  $g_{m3}$  of the input RF stage, with some reasonable hypotheses on transistor dimensions and power consumption.

$$\begin{aligned} L &= 3L_{min} = 1.8\mu m \\ 50\mu m &\leq W_3 \leq 500\mu m \\ I_0 &\approx 5mA \end{aligned}$$

Further, suppositions on bias voltages were made. For example, a voltage equal to  $\frac{3}{5} \cdot V_{dd}$  was supposed to drop between the RF stage's drain and ground, equally divided between M1 and M3 (neglecting the very small voltage drop on  $R_S$ ).

$$V_{SB3} = V_{DS1} = V_{DS3} = 1.5V$$

This allows us to take into account the body effect on threshold voltage of transistor M3. Then we plotted the current and transconductance of the transistor as a function of  $V_{GS}$  and  $V_{DS}$ , that are shown in pictures 11a and 11b.

The largest width  $W_3 = 500\mu m$  (the green curve) was chosen, along with  $V_{GS3} = 1.5V$ , accordingly to the current and transconductance's value, eventually taking the highest values:

$$\begin{aligned} g_{m3} &= 11.9mS \\ \frac{I_0}{2} &= 2.9mA \end{aligned}$$

We moved then to current sink design, M1 and M2. Given the data:

$$\begin{aligned} V_{RS} &= 2.9mA \cdot 10\Omega = 29mV \\ V_{DS1} &= 1.5V - V_{RS} = 1.471V \\ V_{GS1} &= 1.471V \end{aligned}$$

This set of values leads to a width equal to  $W_1 = 373\mu m$  in order to have  $I_0 = 2 \cdot 2.9mA = 5.8mA$  (figure 12).



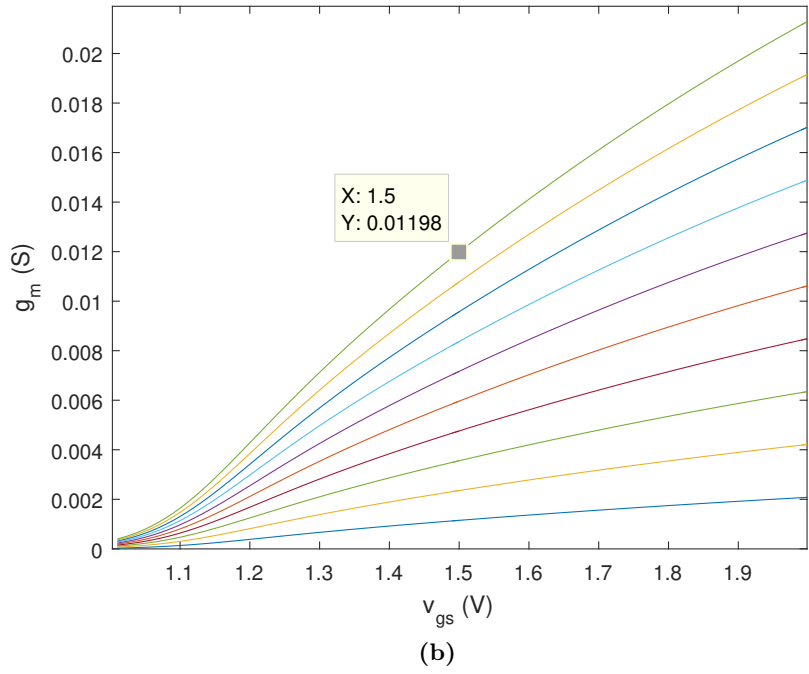
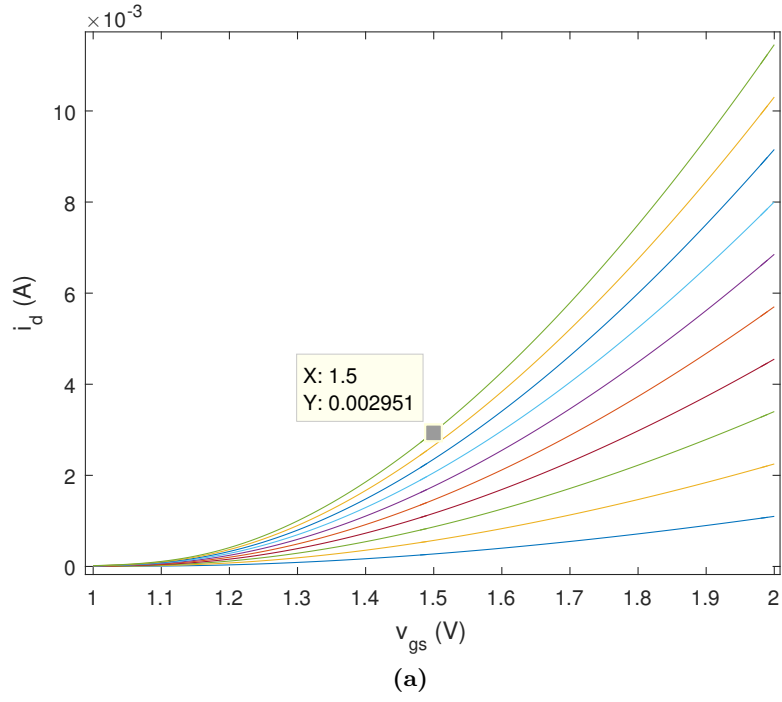


**Figure 11:** a) Drain current versus gate-source voltage of the RF stage, with  $W$  varying from  $50\mu\text{m}$  to  $500\mu\text{m}$ . b) Transconductance versus gate-source voltage of the RF stage, with  $W$  varying from  $50\mu\text{m}$  to  $500\mu\text{m}$ .

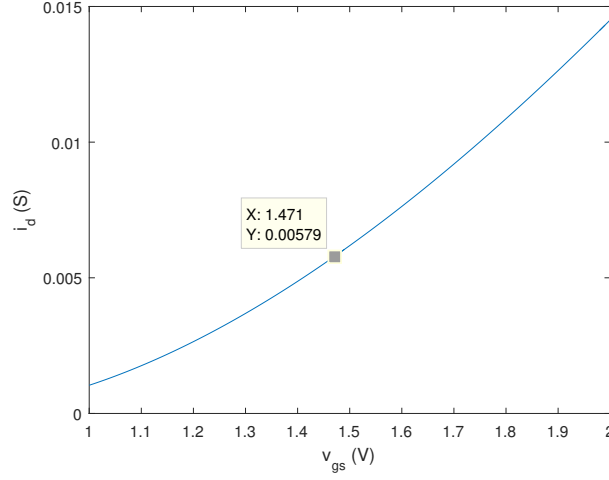


**Figure 12:** Drain current versus gate-source voltage of the bias transistor M1, with  $W=373\mu m$

Finally the LO stage was designed, along with the load resistance  $R_L$  starting from the wanted conversion gain, lowered to  $A_v = 4$  with respect to what we decided in the previous section. Given the analytic expression of voltage conversion gain (Figure 30):

$$A_v \approx \frac{2}{\pi} \left( \frac{R_L}{R_S + \frac{1}{g_{m3}}} \right) = 4$$

The value of  $R_L$  is then determined

$$R_L = A_v \cdot \left( \frac{\pi}{2} \cdot \frac{1}{g_{m3}} + R_S \right) = 577\Omega \quad (56)$$

The drain-to-source voltage of the LO stage,  $V_{DS6}$ , can be thus evaluated as follows:

$$\begin{aligned} V_{SB6} &= V_{DS1} + V_{R_S} + V_{DS3} \\ &= 1.47V + 0.029V + 1.5V = 3V \end{aligned}$$

and

$$\begin{aligned} V_{R_L} &= 2.9mA \cdot 577\Omega = 1.673V \\ V_{DS6} &= V_{dd} - V_{R_L} - V_{SB6} = 327mV \end{aligned}$$

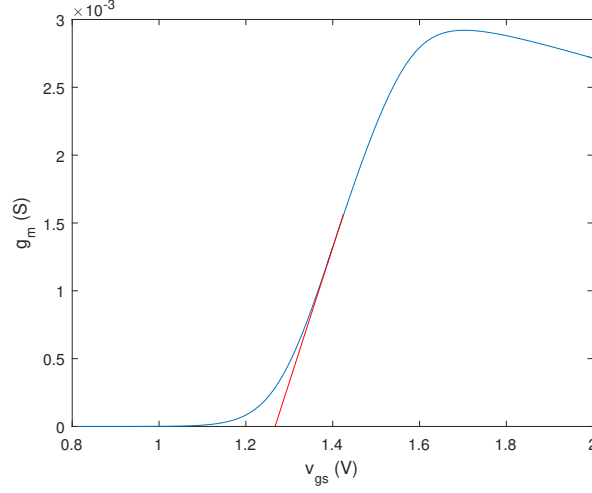


**Figure 13:** Extrapolation of M6 threshold voltage from transconductance versus the  $V_{GS}$  curve. The threshold happens to be at  $1.27V$ .

The LO gate bias voltages must be slightly above the threshold, in order to let the transistors turn on and off with small LO signal variations, deviating rapidly current coming from the RF stage. To accomplish this, the transistor's threshold was extracted from simulation, using the  $g_m$  graph as a function of  $V_{GS}$  (figure 13). Having  $V_{th6} = 1.27V$ , a very small overdrive of  $V_{od6} = 60mV$  was chosen, for the reason reported before, and to assure the stage is not working in triode region. This leads to:

$$V_{GS6} = V_{th6} + V_{od6} = 1.33V$$

Once fixed the gates' voltages and the current flowing in the transistor ( $2.9mA$ , due to the fact that only two transistors of LO stage conduct simultaneously), transistor width  $W_6$  was swept to fulfil precisely this biasing. The followed procedure is the same displayed in figure 11 and the resulting dimensions are:

$$\begin{aligned} W_6 &= 170.3\mu m \\ L &= L_{min} = 0.6\mu m \end{aligned}$$

Only for this stage the minimum channel length was taken, in order to keep small these transistors regardless overdrive small value.

## 4.2 Biasing network design

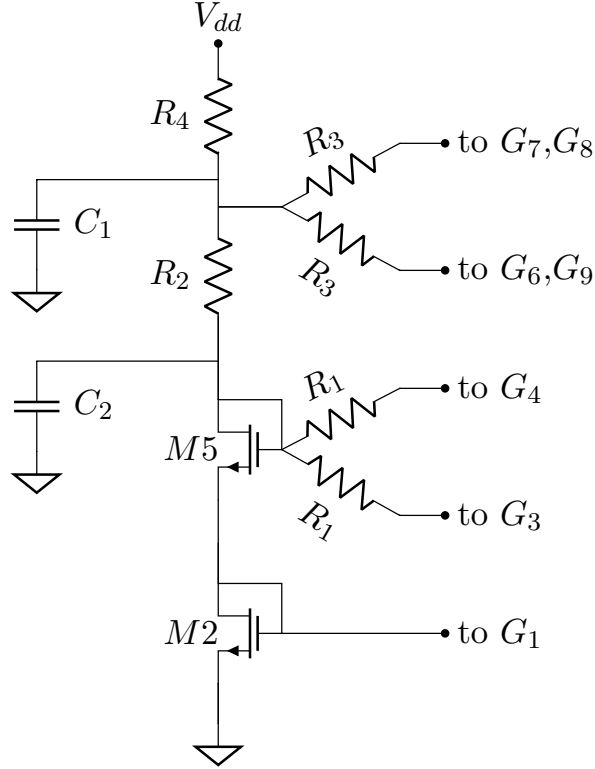


**Figure 14:** Reference biasing network schematic

From the previous section, the bias network specifications required by current sink, RF and LO stage are suddenly imposed:

$$V_{G1} = 1.471V$$

$$V_{G3} = 3V$$

$$V_{G6} = 4.33V$$

The bias network circuit employed is visible in figure 14. The mirroring ratio for the current sink transistor M1 was chosen to be 1 as in section 3. With a transistor length  $L_2 = 1.8\mu m$ , and being  $V_{GS2} = V_{DS2} = 1.471V$  imposed,  $W_2$  has been trimmed in the simulator to sink a current equal to  $I_0 = 5.8mA$ , resulting in:

$$W_2 = 373\mu m$$

In the same way transistor M5 width was set, in order to have a gate voltage  $V_{G5} = 3V$  when stacked above M2:

$$\begin{aligned} W_5 &= 130.45\mu m \\ L_5 &= 0.6\mu m \end{aligned}$$

Minimum length was taken in this case to reduce the transistor's size. The sum of  $R_2$  and  $R_4$  must be such that with total current of  $5.8mA$ , the voltage drop across them is such that  $V_{G5} = 3V$ :

$$R_2 + R_4 = \frac{V_{dd} - V_{G5}}{I_0} = 344\Omega$$

The partition between them must give a bias voltage to LO stage of  $V_{G6}=4.33V$ . This brings to

$$\begin{aligned} R_2 &= 229\Omega \\ R_4 &= 115\Omega \end{aligned}$$

Resistors  $R_1$  and  $R_3$  were chosen to be large enough to isolate biasing network from RF and LO signals respectively, and form a low pass filter along with capacitors  $C_1$  and  $C_2$ . Resistors were thus chosen of the order of some  $k\Omega$ .

$$R_1 = R_3 = 30k\Omega$$

From here, the minimum capacitance to filter out LO signal can be evaluated in order to have a pole at least one decade before working frequency. The output resistance of M5 has been considered negligible with respect to  $R_1$  and  $R_3$ , leading to an equivalent resistance for the low pass filter equal to (neglecting  $g_{m5}$ ):

$$R_{eq} \simeq R_2 || R_4 || \frac{R_3}{2} = 76.4\Omega$$

from which the resulting capacitance:

$$C_1 \geq 10 \cdot \frac{1}{2\pi \cdot R_{eq} \cdot f_{lo}} = 20.8pF \quad (57)$$

$C_1 = C_2$  was chosen for simplicity. Finally a CAD optimization over them was carried on to maximize the gain and minimizing the capacitors' dimensions, leading to the final chosen value of:

$$C_1 = C_2 = 25pF \quad (58)$$



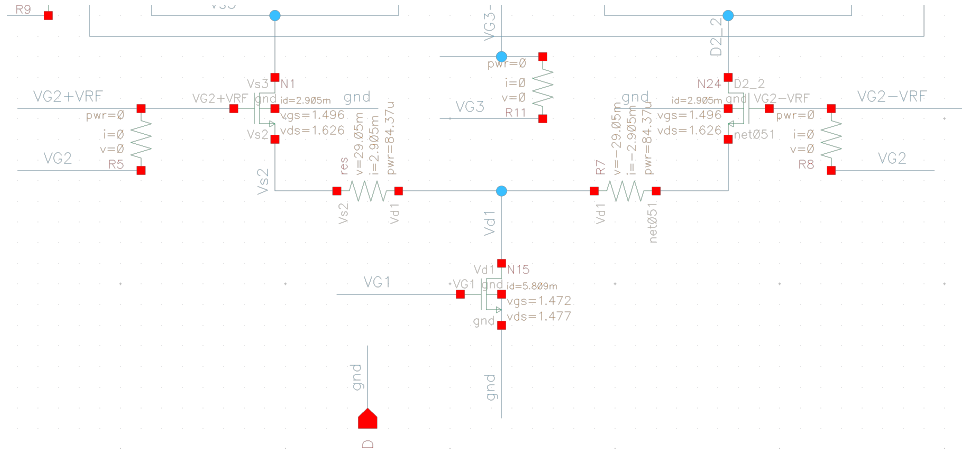


Figure 16: Close up view on current sink and RF stage

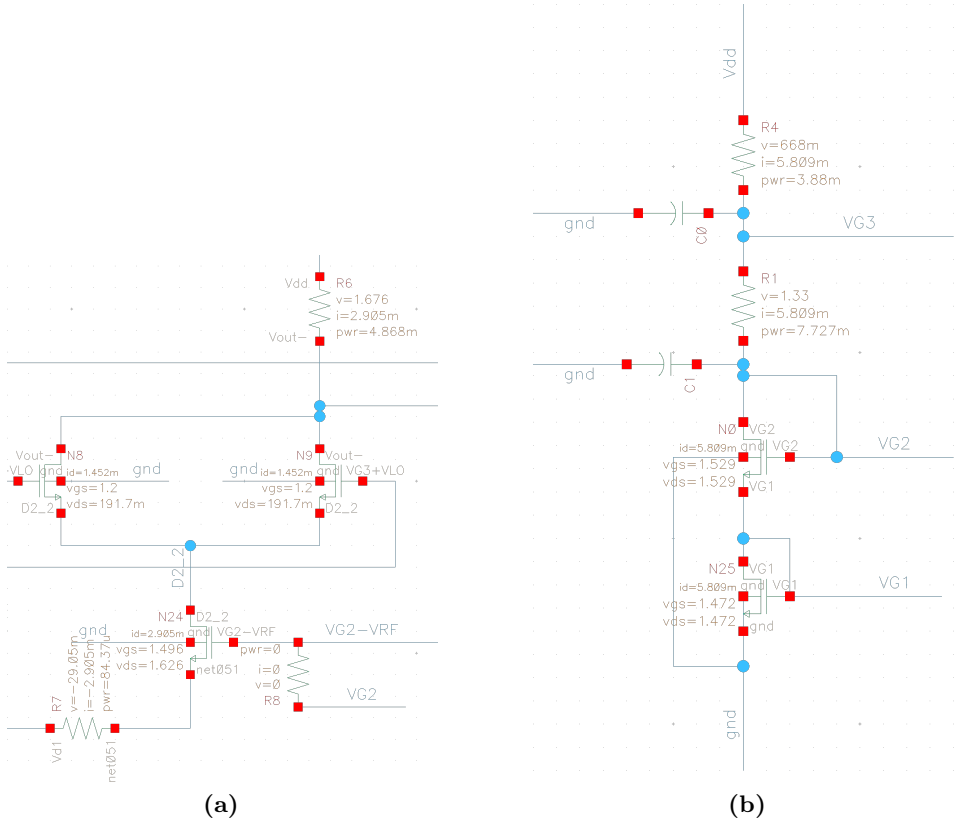


Figure 17: a) Close up view of LO stage. b) Close up view of LO stage

### 4.3 Validating design of the bias point

Designed circuit has been drawn in Cadence to test it entirely. The complete test circuit is shown in figure 15, after dc operating point simulation. As it can be seen from the close-up figure 16 bias voltages and current of the current sink M1 (N15 in Cadence schematic) are practically the same of the ones obtained in the design. Same thing can be stated for RF and LO stage in figure 17 and for the biasing network (figure 17). Dynamical analyses for the circuit in figure 15 have been moved in this treatise to the final chapter. In the next section circuit layout is described.







## 5 Layout of the Gilbert Cell

The overall layout was carried on with a view to:

- reducing technology gradients using common centroid, interdigitated or multi-finger structures;
- placing components all in the same direction for a uniform error affection;
- reducing border effects with dummy elements;
- minimizing encroachment errors with same-length transistor fingers;
- limiting substrate noise with guard rings;
- avoiding connections which could lead to crosstalk;
- minimizing metal changes in the routing process;
- aiming a compact structure.

### 5.1 Differential RF stage

A careful attention has been paid to the layout of differential pairs like the one of RF stage. Since it's desirable to have the most symmetric input stage a common centroid configuration has been employed, following a structure sketched as in Figure 18.

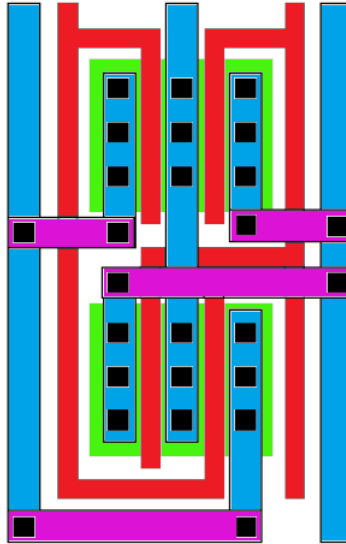


**Figure 18:** Common centroid structure used for differential RF stage

This minimizes errors due to process gradients within the planar structure. Dummy elements were also placed next to the four transistors at the edges to guarantee a uniform dopant concentration of the inner transistors.

Dummy MOSFETs' drain and source are tied together and then short circuited to source. The transistor length of the differential pair has been divided to form multi-finger transistors, such that the whole structure results as square and compact as possible. This was intended again for the purpose of reducing gradients and with a glance forward to the overall mixer layout's compactness. The final layout of differential RF pair is shown in Figure 19.

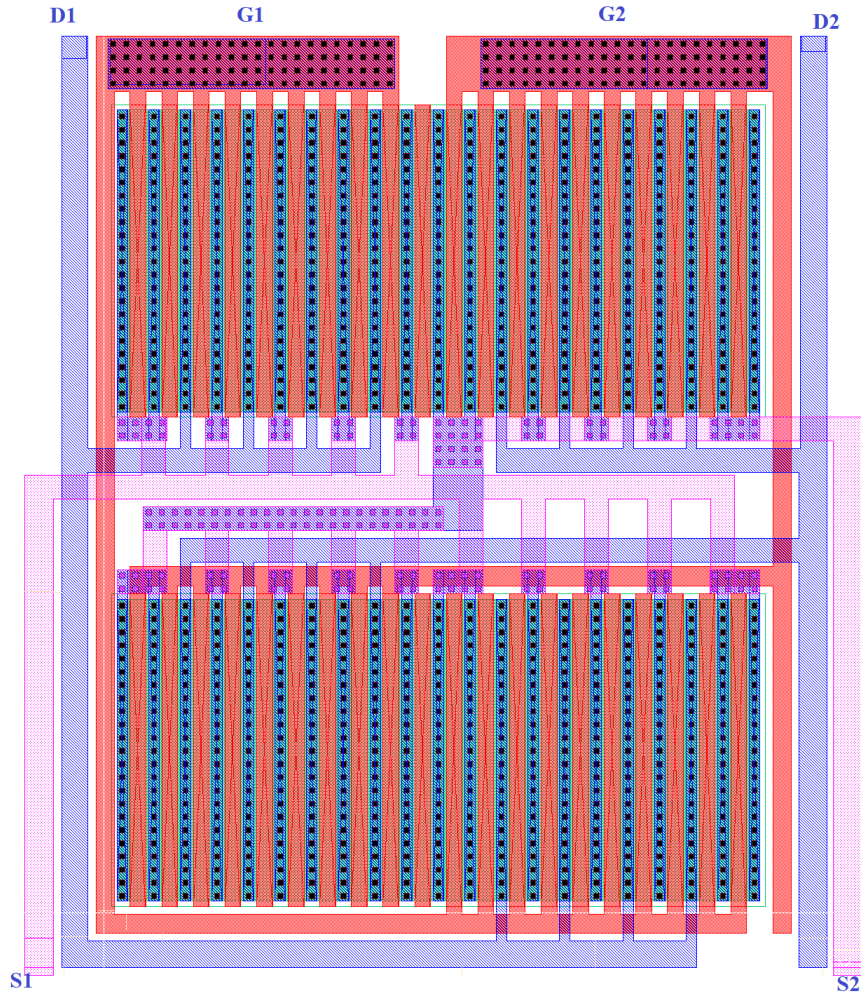


**Figure 19:** Complete layout of RF differential transistor

## 5.2 Differential LO stages

The two differential LO stages have been designed trying to prevent the same mismatch causes seen for the RF stage. Two common centroid structure were drawn at first. Being the transistor wide, multi-finger structure was employed also here to have an almost-square layout along with dummy elements. Attention has been paid in so that the two LO pairs could be easily stack above the RF stage with the same width. Secondly, we opted for a merging of the two common centroid LO layouts in a more compact tiled layout. The gate disposal simplifies the access to these nets from the signal capacitors in the global layout. Final LO layout is shown in Figure 20 .

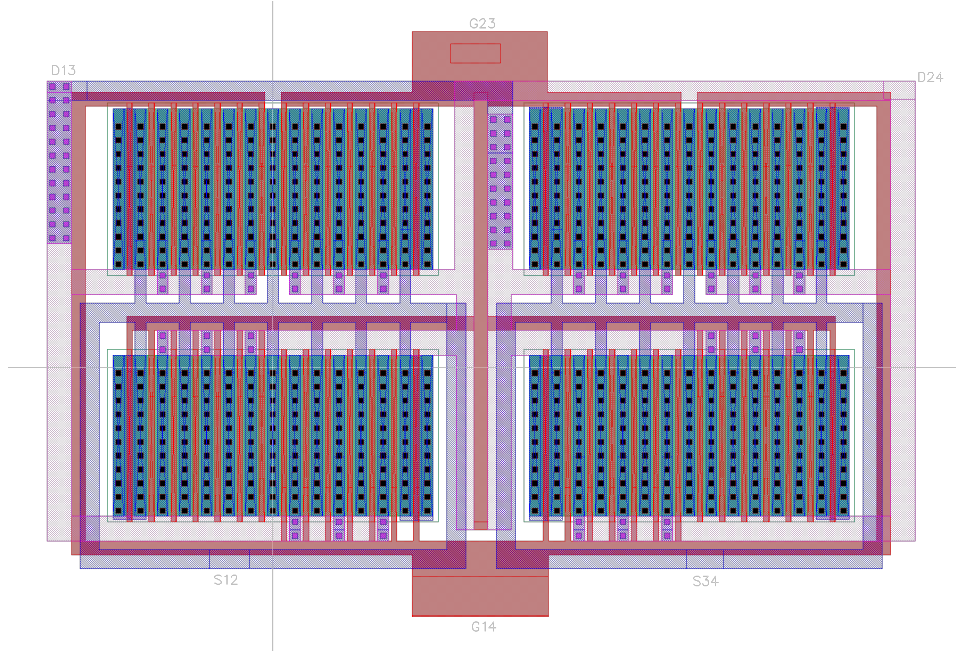


**Figure 20:** Complete layout of LO differential stages

## 5.3 Current mirror and diode connected transistor

Current mirror employs an interdigitated structure similar to the one visible in Figure 21.

Since fingers are all the same size the current ratio is independent from encroachment width. Dummy transistors was included to reduce border effects, and source connections on both top and bottom sides have been added for a small source resistance. The weak branch transistor's drain has been tied together to the gate with an array of contacts. The final layout for current mirror is visible in Figure 21.



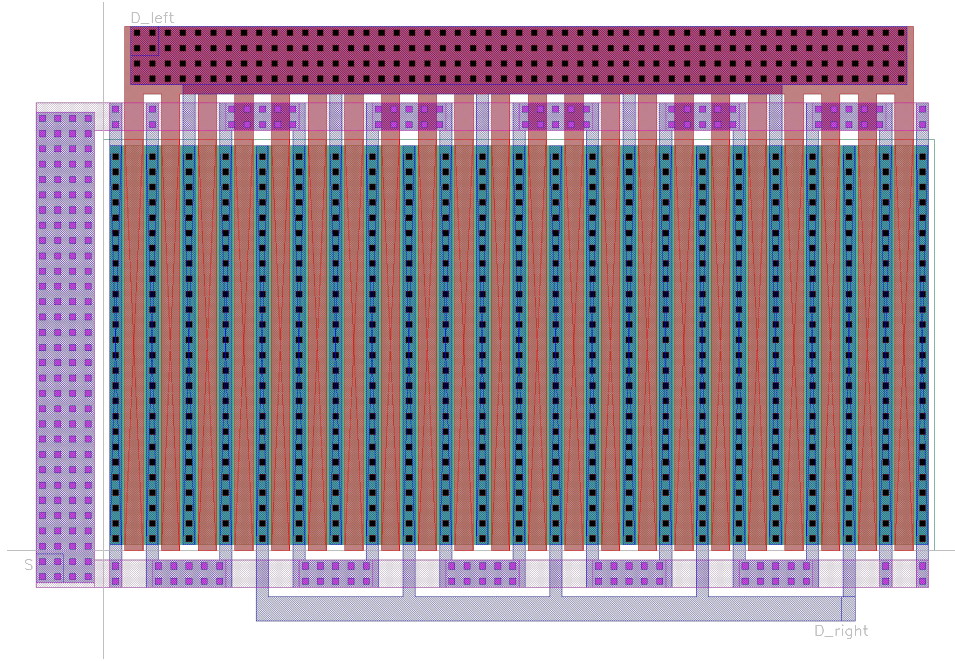


**Figure 21:** Complete layout of current mirror

Concerning the diode-connected transistor M5, interdigitated structure was implemented. Dummy transistors are placed aside whereas an array of contacts to minimize series resistance between gate and drain has been added. Final layouts and highlighted nets are visible in Figure 22.

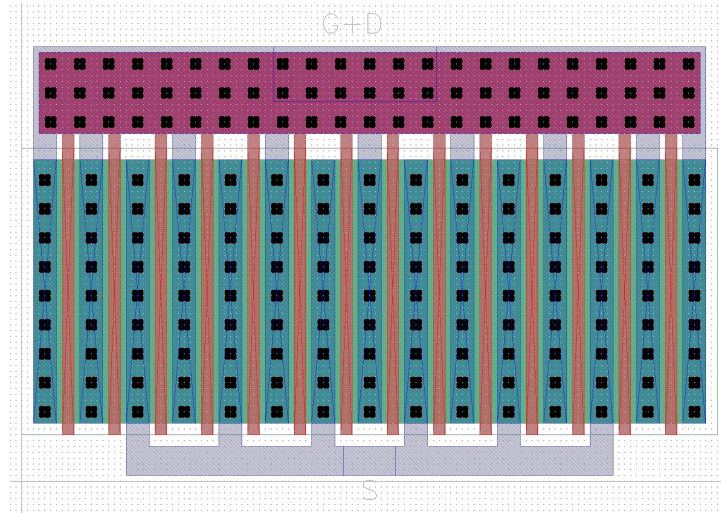


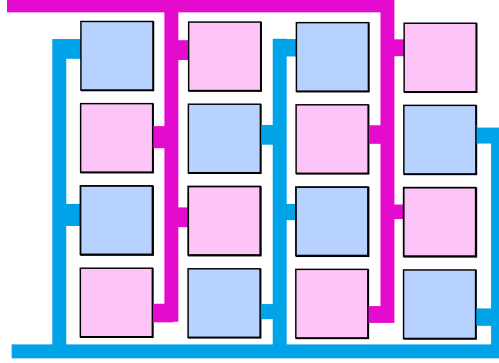
**Figure 22:** Complete layout of M5 transistor

**Table 2:** MOSFETs CAD parameters

| Parameter      | M <sub>1,2</sub> | M <sub>3,4</sub> | M <sub>5</sub> | M <sub>6,7,8,9</sub> |
|----------------|------------------|------------------|----------------|----------------------|
| m              | 10(+1)           | 18(+2)           | 12(+2)         | 12(+2)               |
| w* [ $\mu m$ ] | 39.15            | 34.35            | 13.65          | 17.55                |
| W [ $\mu m$ ]  | 391.15           | 618.3            | 163.8          | 210.6                |
| L [ $\mu m$ ]  | 1.8              | 1.8              | 1.8            | 0.6                  |
| y [ $\mu m$ ]  | 61.5             | 126              | 25.2           | 56.85                |
| x [ $\mu m$ ]  | 87.75            | 99.45            | 35.55          | 87.6                 |

## 5.4 Capacitors

**Bias capacitors** Bias capacitors have been designed using two configurations of common centroid layout. A simplified version of the layout structure implemented is drawn in Figure 23.

**Figure 23:** Bias capacitors layout structure

Even if no exact ratio between the two capacitors is needed, a modular geometry, made by equal squares, was used. This minimizes undercut effects, and the square shape reduces border errors. In order to reduce the area, capacitor units were designed using poly1 and poly2 (elec) layers, which give the maximum capacitance per unit area available with this technology kit. A dummy capacitor frame was placed around to minimize border effect. All the capacitors lie above an n-well, whose purpose is to minimize fringing field leakage. This n-well is tied to  $V_{DD}$  potential. The final layout with highlighted nets is visible in Figure 24.

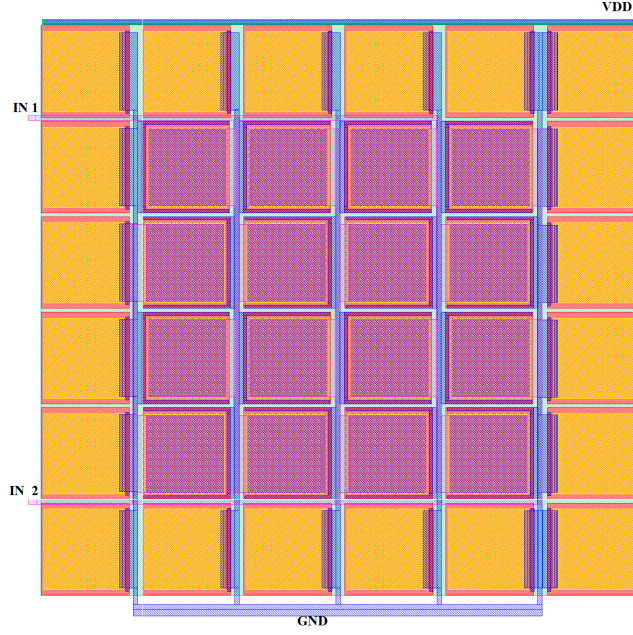


**Figure 24:** Full layout of  $C_{bias}$  capacitors

**Signal capacitors** Since these capacitors resulted to be very space demanding due to capacitance value, a multi-layer capacitor was tried to be built alternating poly and metal layers. Unfortunately this idea was soon abandoned due to the *rule 11.6 of SCMOS* rules, which does not allow unrelated metal layer over poly2. The most practical solution proven to be using poly1-to-poly2 capacitance in a common centroid structure. This time matching is more important with respect to bias capacitors, because we want signal coming to the differential stages pass through strongly symmetrical paths. A simplified version of the common centroid structure implemented is shown in Figure 25.

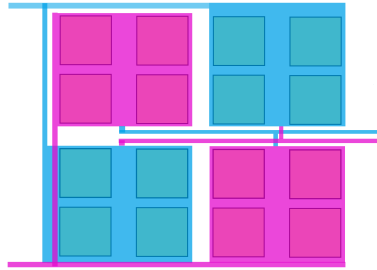


**Figure 25:** Common centroid structure of the signal capacitors



Since this is a high frequency path to reduce series resistance and inductance, metal plates with contacts were placed all over the square unit capacitors. Dummy short circuited elements were positioned all around the capacitor as well. An additional n-well connected to  $V_{DD}$  surrounds the capacitor to reduce fringing field leakage. The overall capacitance layout with highlighted nets is visible in Figure 26.

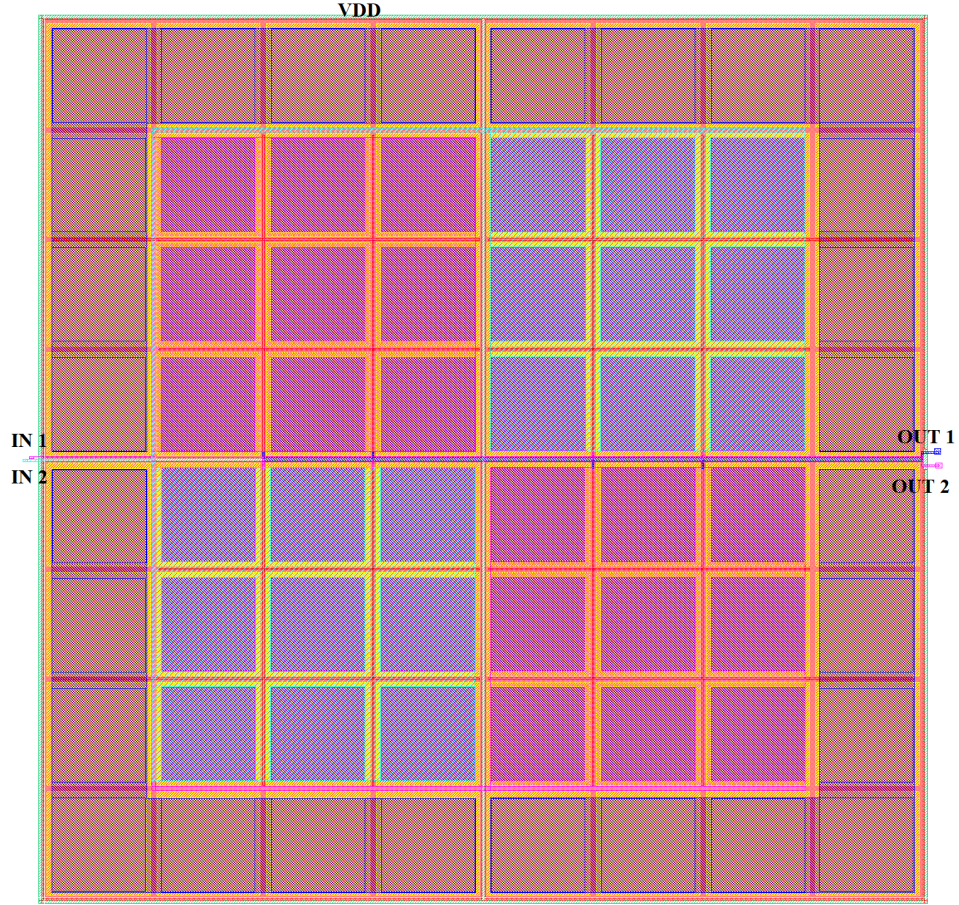


**Figure 26:** Full layout of  $C_{signal}$  capacitors

**Table 3:** Capacitors CAD parameters

| Parameter   | $C_{bias}$ | $C_{signal}$ |
|-------------|------------|--------------|
| $y [\mu m]$ | 448.65     | 678.45       |
| $x [\mu m]$ | 472.5      | 480.25       |
| $C [pF]$    | 25.9       | 90.1         |

## 5.5 Resistors

Two kinds of resistors have been implemented in this layout, both of them are described in the following paragraphs.

**N-well resistors** Resistors fabricated in n-well have worse tolerance, but an higher sheet resistance. That's the way this kind of resistor was chosen to implement biasing resistors  $R_1$  and  $R_3$ , which are, as a matter of fact, very large in absolute value, but their tolerance is not too important. We can thus have smaller layout adopting n-well layout. Resistors were split in modular structures with the common centroid fashion to reduce differences between  $R_1$  and  $R_3$ . Due to the fact that this resistors are very close to the mixing stage, a guard ring connected to ground has been included to prevent substrate noise being injected through the biasing network. The final layout obtained for  $R_1$  and  $R_3$  resistor is visible in 27.

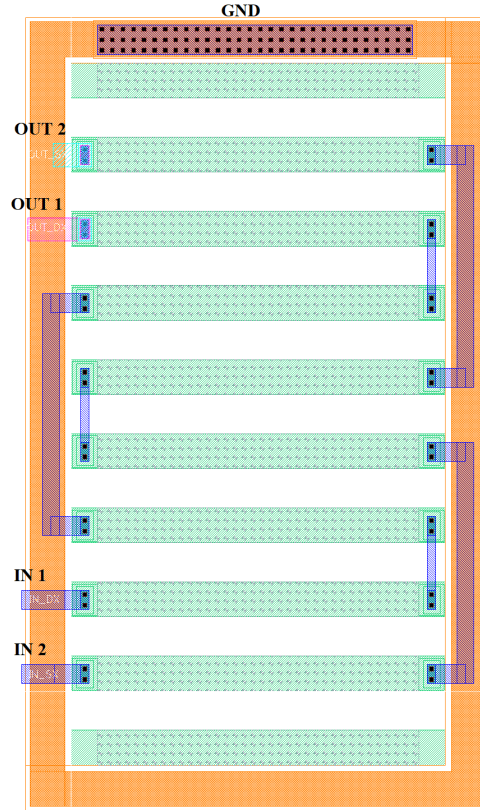


**Figure 27:** Layout of  $R_1$  and  $R_3$  resistors

**Poly silicon resistors** Since other resistors are smaller than  $R_1$  and  $R_3$ , poly has been employed to build them, taking advantage of their higher

precision but smaller sheet resistance. All of them were drawn in common centroid structure, except for  $R_4$  (due to its small value), and dummy elements on both sides were always used. Final layouts for these resistors are shown in 28a, 28b, 28c, 28d (dimensions are not in scale).

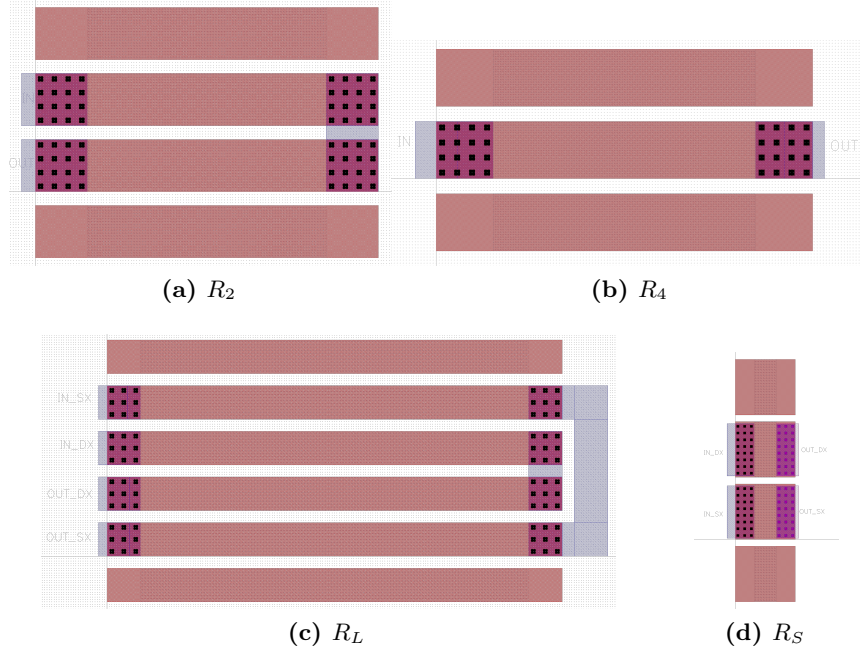


**Figure 28:** Poly resistors layout

**Table 4:** Resistors CAD parameters

| Parameter              | $R_{1,3}$ | $R_2$ | $R_4$ | $R_L$ | $R_S$ |
|------------------------|-----------|-------|-------|-------|-------|
| $y$ [ $\mu m$ ]        | 112.05    | 27.45 | 20.1  | 32.4  | 54    |
| $x$ [ $\mu m$ ]        | 66.3      | 37.35 | 37.65 | 63    | 13.35 |
| $h$ [ $\mu m$ ]        | 4.95      | 5.7   | 5.7   | 4.2   | 12.45 |
| $w$ [ $\mu m$ ]        | 46.5      | 26.1  | 26.25 | 48.6  | 4.95  |
| $m$                    | 4         | 2     | 1     | 1     | 1     |
| $R^*$ [ $\Omega$ ]     | 7545      | 114.5 | 115.1 | 289.3 | 9.94  |
| $R_{tot}$ [ $\Omega$ ] | 30180     | 229   | 115.1 | 289.3 | 9.94  |



## 5.6 Putting together the layout

The layout has been organized in order to minimize the occupied surface area. The final configuration can be seen in Figure 30. Components have been placed to shorten interconnections, emphasize symmetries for matching and to make paths as equal as possible for high frequency signals. Body contacts where placed all around the circuit where possible, and then connected to ground, in order to capture free charges in the substrate reducing noise. A close up vision of the complete layout, without capacitors, is visible in Figure 29.

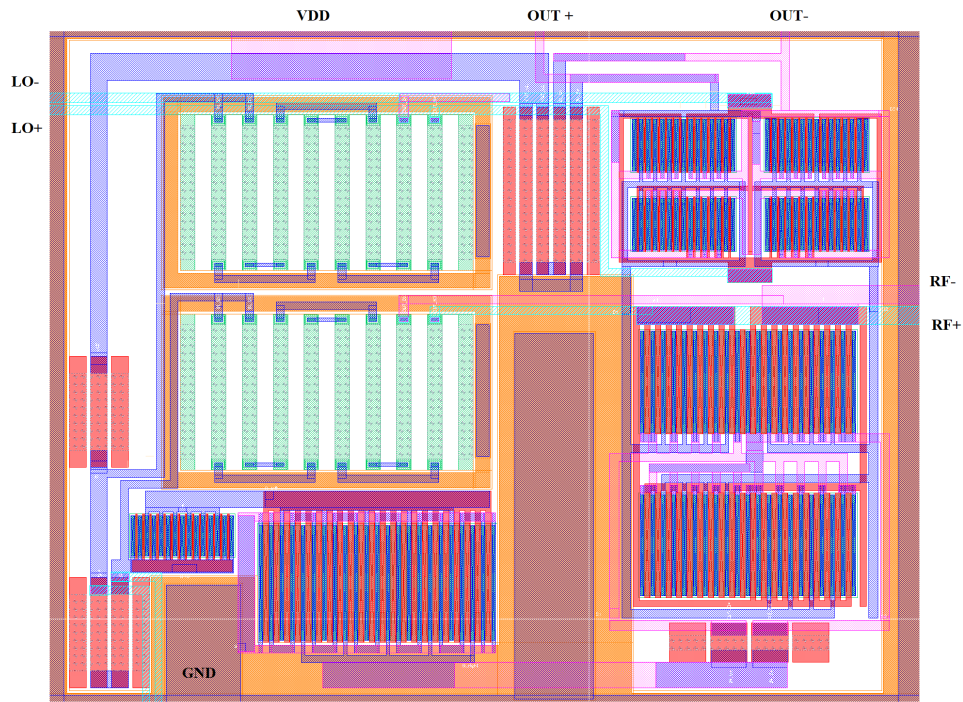


**Figure 29:** Close up of the complete layout

The whole occupied area is approximately  $0.7mm \times 1.8mm$  and it's mainly due to size of the signal capacitors. Such a big area can be also justified with the fact that the used technology is not well suited for this kind of RF design, and it was carried on mainly with the scope of learning how to layout a circuit.

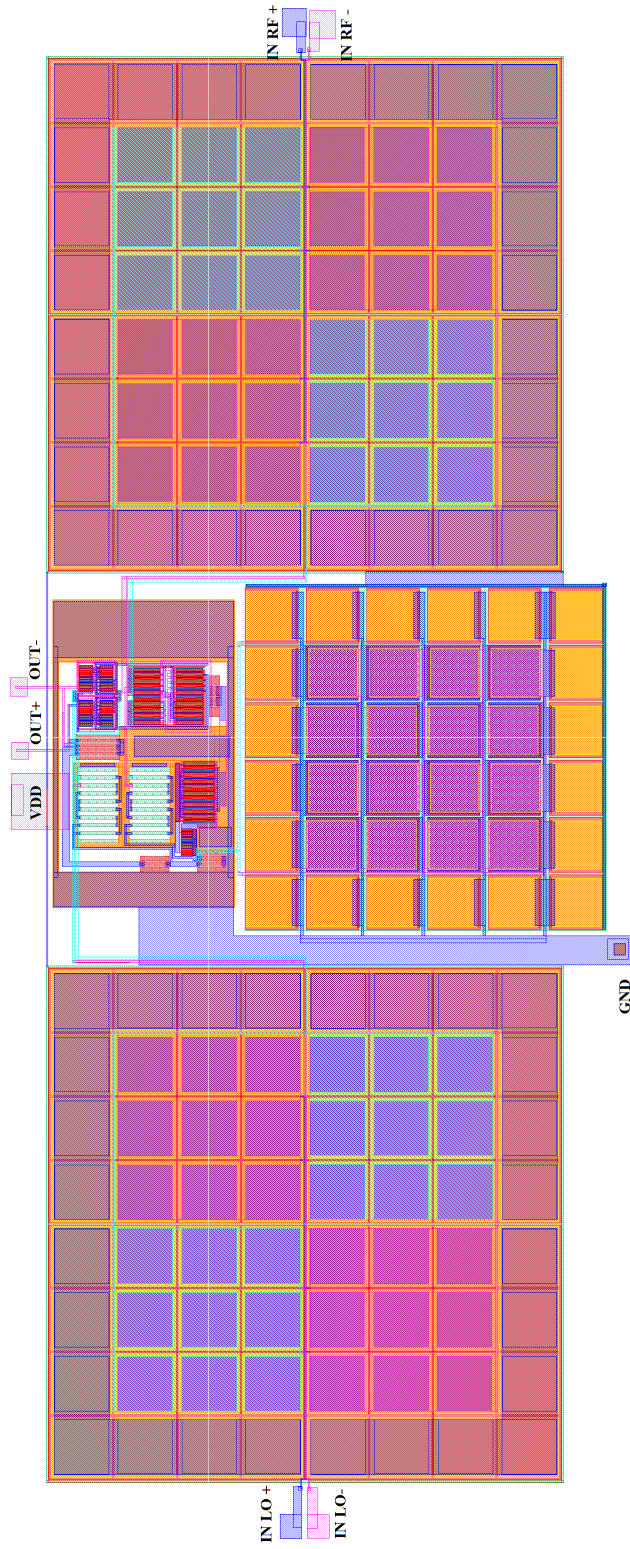


**Figure 30:** Layout of the complete Gilbert balanced mixer



## 6 Simulation vs schematic comparison

### 6.1 Simulation setup

Last step was to characterize the layout and evaluate its behaviour in comparison with the schematic. The carried on analysis are the following:

- Time domain output mixed signal and spectral components;
- Oscillator amplitude to maximize output component;
- Conversion gain and 1dB compression point;
- Single tone IIP<sub>3</sub>;
- Two tone IIP<sub>3</sub>;
- Bandwidth of RF stage (output node filtering of output signal, current mixing);
- Static power dissipation;

All the analysis were developed using monochromatic signals at frequencies 100MHz for LO, 110MHz for RF, and considering the mixer working in down-conversion (10MHz IF frequency).

To compare schematic and layout we used the set-up proposed in figure 31, that includes:

- The symbols related to mixer's schematic and layout under test.
- Input AC signals generators. Those elements are connected to ideal baluns (figure 32) in order to simulate a perfect  $50\ \Omega$  impedance matching condition, producing differential inputs also. Two LO generators are used to customize the optimal carrier power level entering in each mixer.
- Power supply net, implicitly connected to both layout and schematic.
- Mixer's loads, represented by  $50\Omega$  resistors connected to unitary gain driven generator. This is used both for ideal impedance matching purposes and to convert differential (balanced) output from mixers to single-ended (unbalanced).

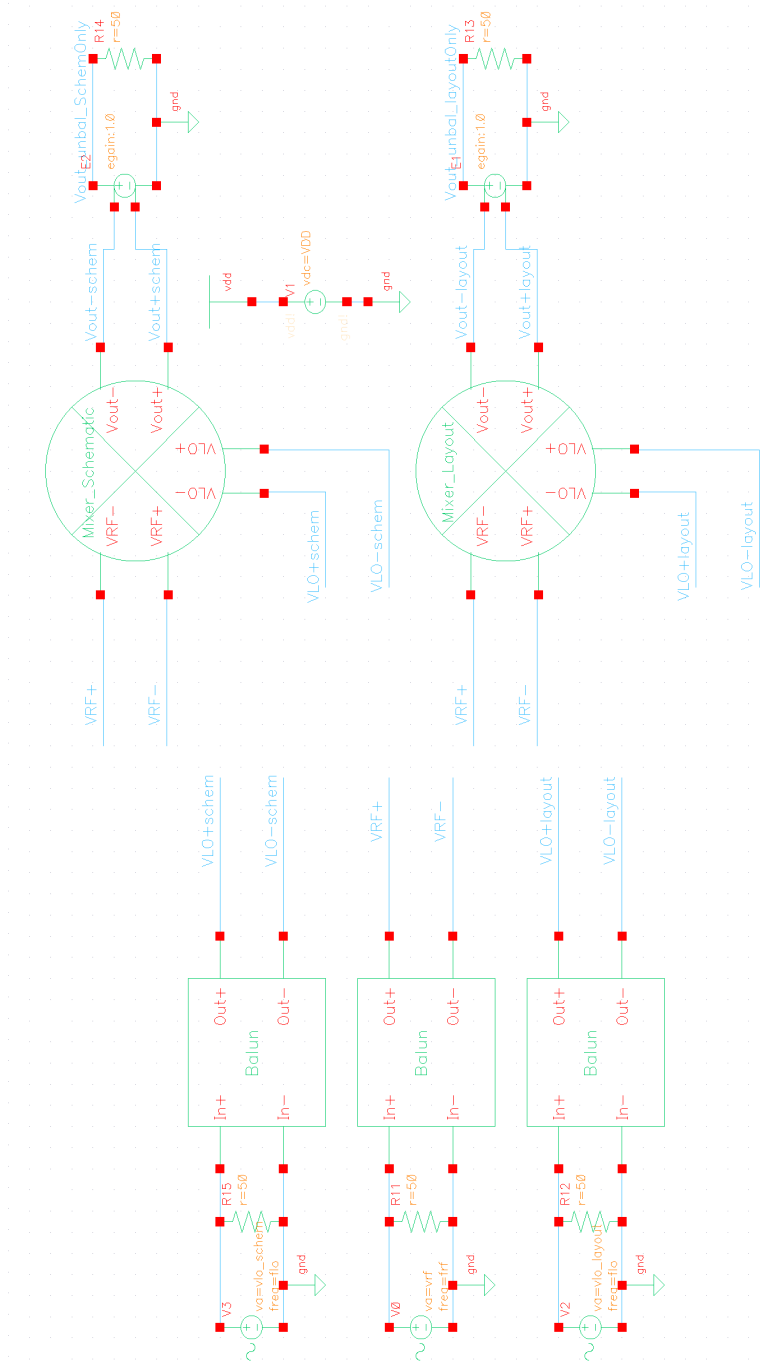


**Figure 31:** Simulation set-up.



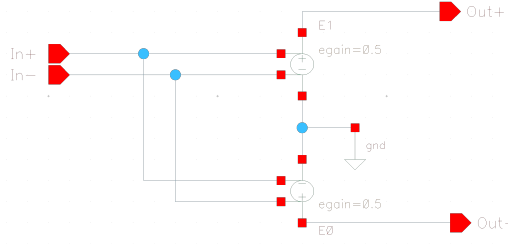


**Figure 32:** Balun schematic.

## 6.2 Bandwidth evaluation

Being a mixer a non-linear circuit, we cannot evaluate the bandwidth computing Bode's diagram by means of AC small signal analysis. A first, rough, idea about each transistors performances can be obtained by measuring the transition frequency. Current gains have been simulated for both RF and LO stages, with bias operative condition previously found (figure 33a), having:

$$f_T|_{RF} = 9.43GHz$$

$$f_T|_{LO} = 1.12GHz$$

These frequency values are not directly related to the circuit's actual speed, however a limiting upper bound can be used as reference (maximum frequency ten time lower than  $f_T$ ).

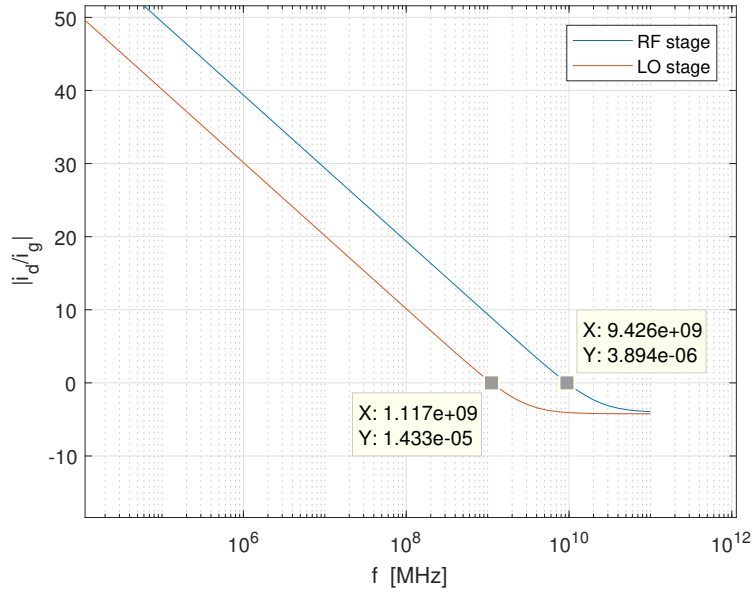
Figure 33b shows the conversion gain as a function of RF input signal. We set  $f_{LO} = f_{RF} - 10MHz$ , in order to keep constant  $f_{IF}$ . As it appears our working point presents a small decreasing from maximum gain, it is quite distant from the -3dB point though (almost 2 octaves lower).

If we consider  $f_{3dB}$  as the maximum operative frequency we that the circuit presents surprising performance, since this point gets very close to transition frequency.

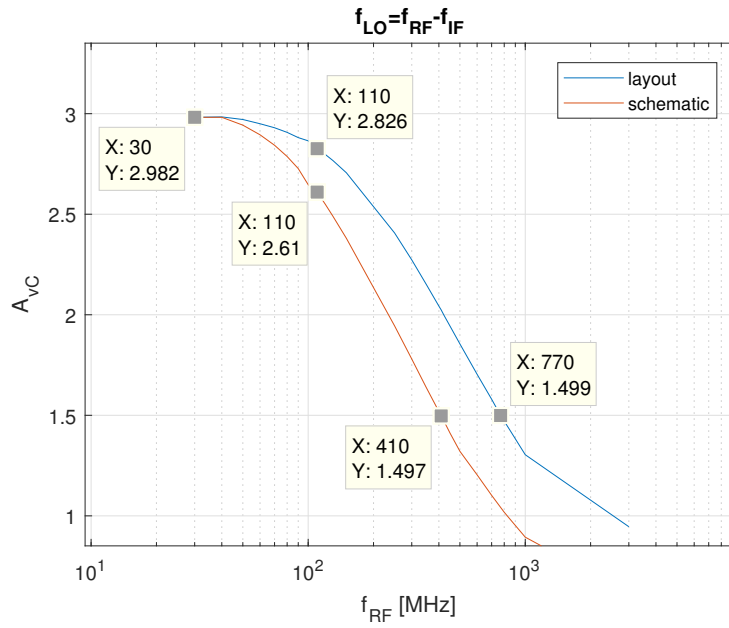
However we never considered high frequency reactive behaviour, because the model provided by the CAD tool was not intended to take into account the full set of parasitics, which play an important role at RF. The circuit physical implementation would be surely worse (mainly due to connection and package).

Pretending that our simulation is accurate, this assumption of LO and RF frequency represents the worst case operative condition.

Our assumptions on LO and RF frequencies were thus considered adequate, since represent the worst-case performances of the mixer. Maximum operating frequency could thus be improved reducing output node capacitance (for example using a folded cascode configuration for the mixing stage).



(a) current gain



(b) Conversion gain vs bandwidth

**Figure 33:** a) transition frequency and b) mixer bandwidth evaluation. In figure b it is possible to identify the constant gain region ( $f_{30\text{MHz}}$ ), gain value for this project ( $f_{110\text{MHz}}$ ) and -3dB points for RF and LO stages respectively.

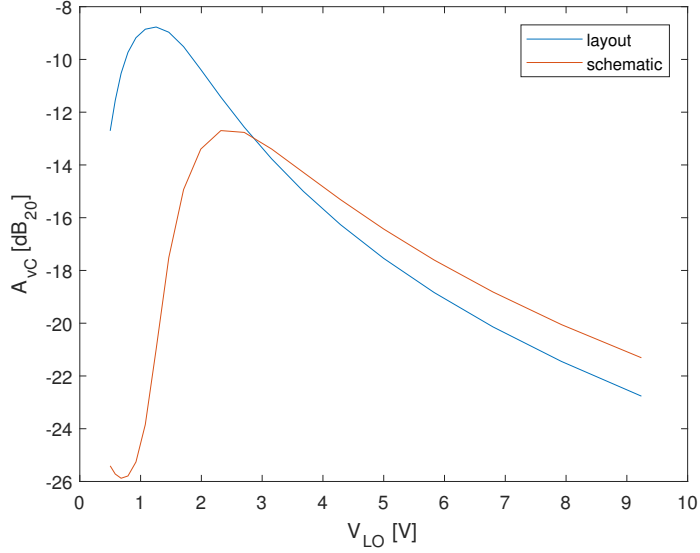
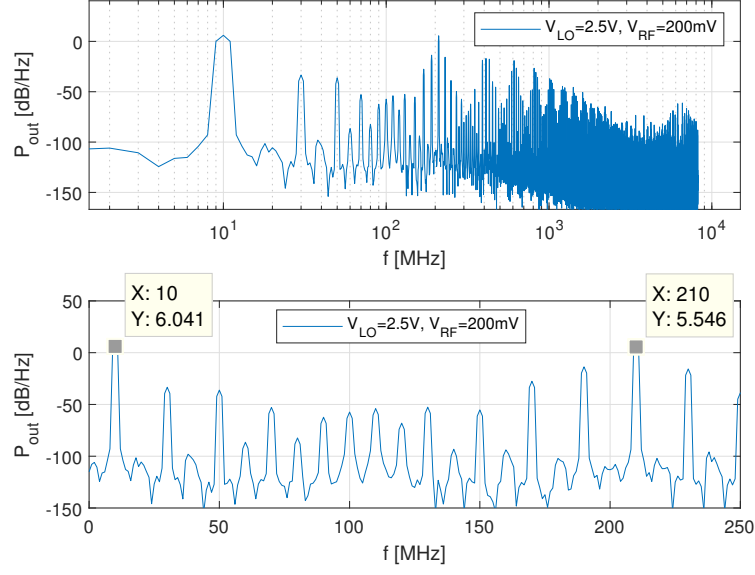


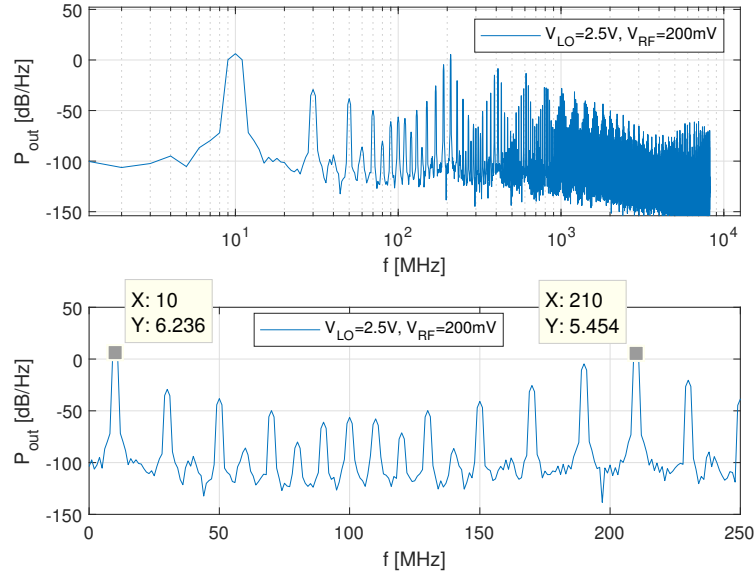
**Figure 34:** Conversion gain vs  $V_{LO}$ .

### 6.3 Maximum conversion gain vs LO

Input LO signal was swept to find the optimum value that maximizes output voltage at IF. The analysis has been carried on for both schematic and layout circuit. Voltage  $v_{rf} = 200mV$  was kept constant during the analysis, and output amplitude at 10MHz was divided by LO amplitude such that the peak corresponds to the maximum LO amplitude for which IF output power saturates. Results are shown in figure 34. It can be noticed that schematic and layout reach their maximum for different values of LO signal, 2.5V and 1.23V respectively. In general it can be noticed that layout has an higher gain than the schematic. Trying to change  $v_{rf}$  amplitude very tiny changes in peak output voltage where found, so the first analysis was kept as a quite good estimation for optimum LO peak voltage. From now on all the comparison between the two circuits have been made imposing the optimum LO voltage for each circuit.



(a) layout



(b) schematic

**Figure 35:** Discrete Fourier transform: double balanced differential output with  $v_{RF}=200mV$ ,  $f_{RF}=110MHz$ ,  $v_{RF}=1.23mV$ ,  $f_{LO}=100MHz$ , cosine squared smoothing function. a) layout, b) schematic

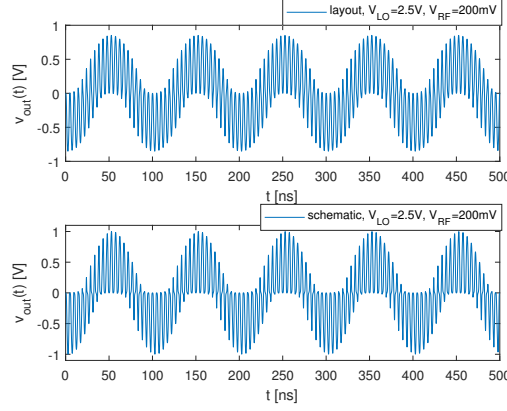


**Figure 36:** Time domain waveforms: double balanced differential output with  $v_{RF}=200\text{mV}$ ,  $f_{RF}=110\text{MHz}$ ,  $v_{LO}=1.23\text{mV}$ ,  $f_{LO}=100\text{MHz}$ .

#### 6.4 Time domain mixed signal

The mixed output signal with  $v_{rf}=200\text{mV}$  and  $v_{lo}=1.23\text{V}$  is visible in figure 36. The waveform looks like the expected one from literature. Applying the discrete Fourier transform to the if signal we found the graph seen in figure 35a and 35b. It's clearly visible the intrinsic capability of double balanced mixer of rejecting input components at  $v_{lo}=100\text{MHz}$  and  $v_{rf}=110\text{MHz}$ .

#### 6.5 Conversion gain and 1dB compression point

Keeping optimum LO amplitude, RF's voltage was swept in order to see how output power at IF frequency increases with input power at RF. Reference port for all power measurement has been chosen to be  $50\Omega$ .  $P_{IF}$  as a function of  $P_{RF}$  conversion gain is shown in figure 37 for both schematic and layout, whereas gain can be seen in figure 38. From simulation we have:

$$\begin{aligned} A_{vC}|_{layout} &= 2.926 \\ A_{vC}|_{schematic} &= 2.675 \end{aligned}$$

Extrapolation of 1dB compression point was carried on, leading to the measurement of RF power for which the gain drops of 1dB equal to

$$\begin{aligned} P_{RF,in}|_{layout} &= -2.3\text{dB}_m \\ P_{RF,in}|_{schematic} &= -4.8\text{dB}_m \end{aligned}$$

then, respectively for schematic and layout, corresponding to the voltages:

$$\begin{aligned} V_{RF,in}|_{layout} &= 172\text{mV} \\ V_{RF,in}|_{schematic} &= 128\text{mV} \end{aligned}$$

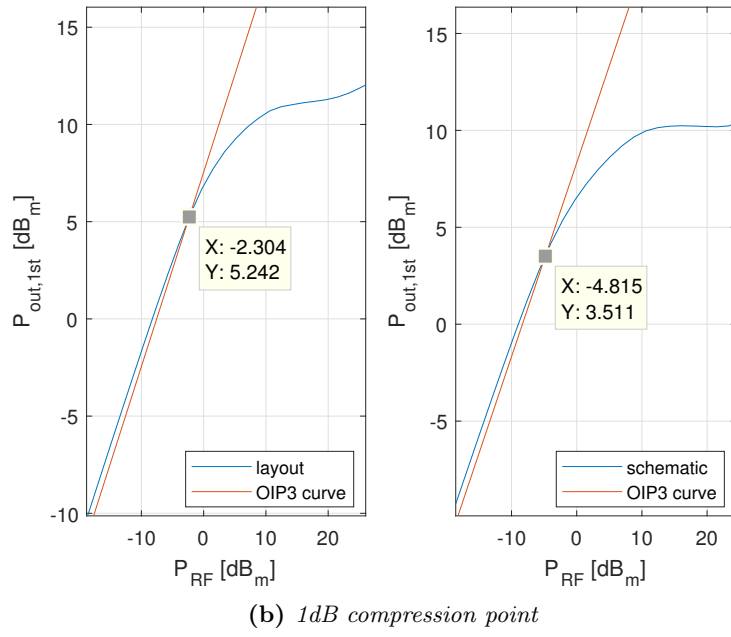
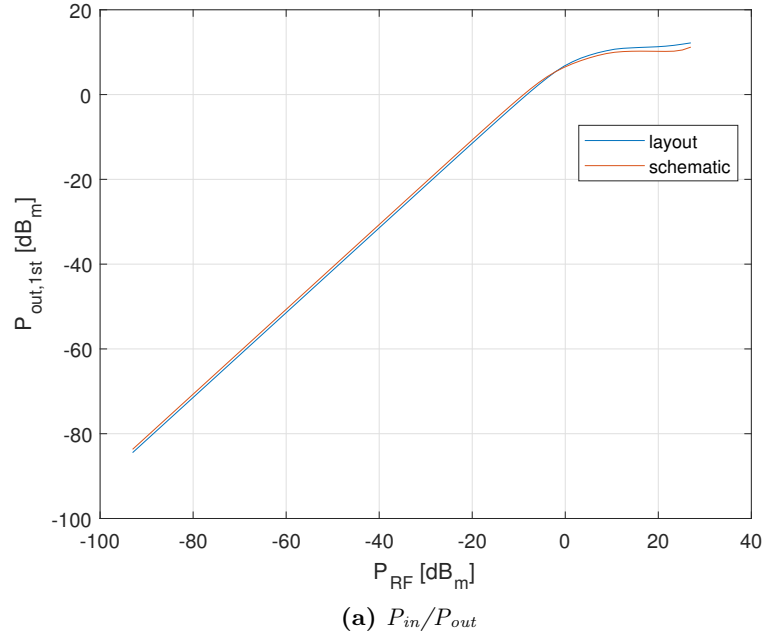


**Figure 37:** a)  $P_{in}/P_{out}$  and b) 1dB compression point, one-tone analysis.

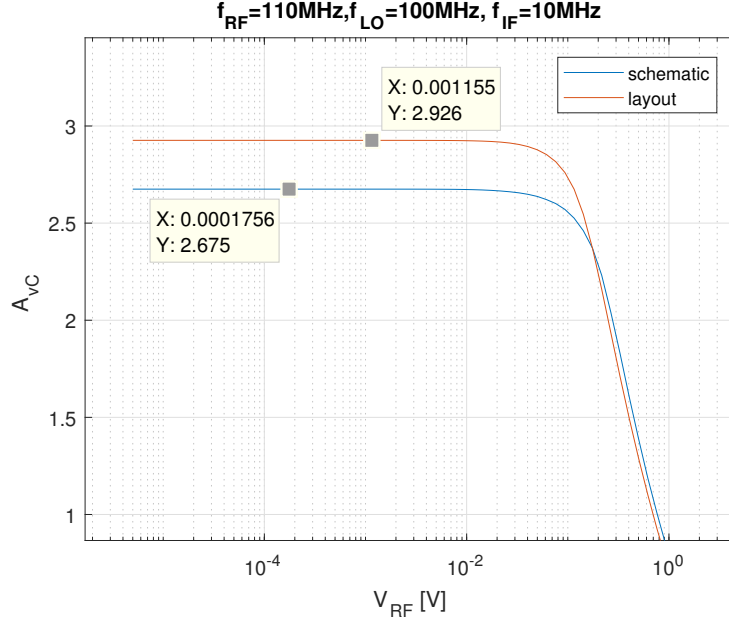


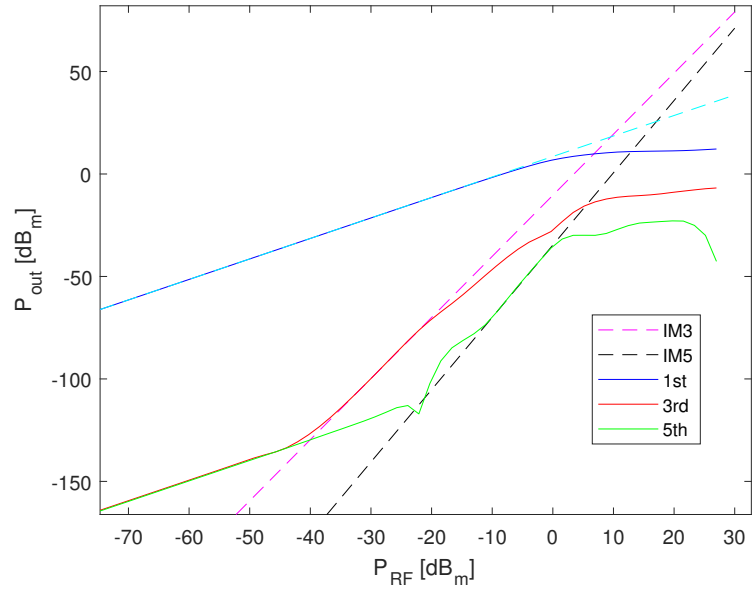
**Figure 38:** Conversion gain vs  $V_{RF}$ .

## 6.6 Single tone third order distortion

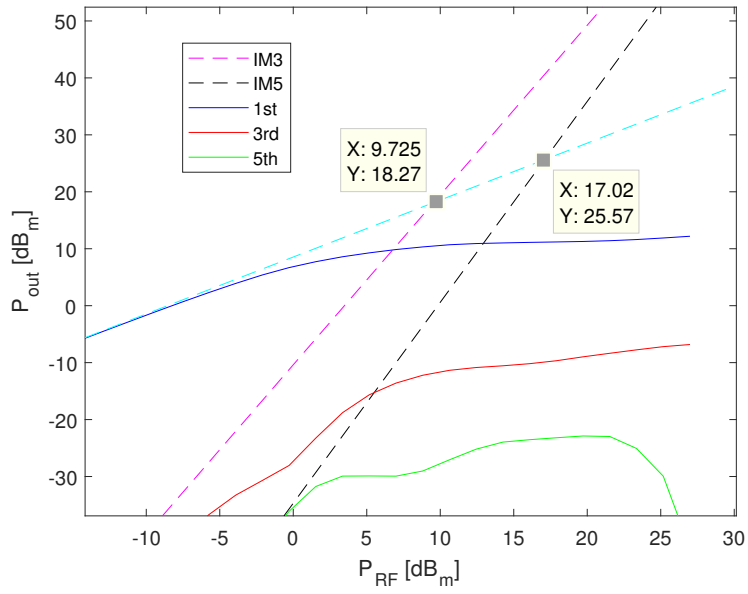
Using single tone RF signal, power on the third harmonic with respect to the IF tone has been measured. Third order distortion is in fact the first contribution to non-linearities(**SELFREFERENCE**). The typical cubic behaviour with respect to the linear one of the conversion gain can be easily seen in logarithmic scale, shown in figure 39 for the schematic and in figure 40 for the layout. Linear regression was applied to the curves to find the third order intercept points for both schematic and layout test benches. Values of IIP3 and OIP3 thus found for both layout and schematic are reported in table 2. From where it appears that the layout extracted introduces less third order distortion than schematic, fifth order distortion looks higher at lower input power though.

**Table 5:** IIP3 and IIP5 in one tone analysis.

| Parameter Name | Schematic | Layout | unit   |
|----------------|-----------|--------|--------|
| $IIP_3$        | 9.73      | 10.4   | $dB_m$ |
| $OIP_3$        | 18.3      | 19.7   | $dB_m$ |
| $IIP_5$        | 17.0      | 9.13   | $dB_m$ |
| $OIP_5$        | 25.6      | 18.5   | $dB_m$ |



(a) harmonics power



(b) detail in IIP3 and IIP5

**Figure 39:** Harmonics power, IIP<sub>3</sub> and IIP<sub>5</sub> in schematic, one tone analysis.



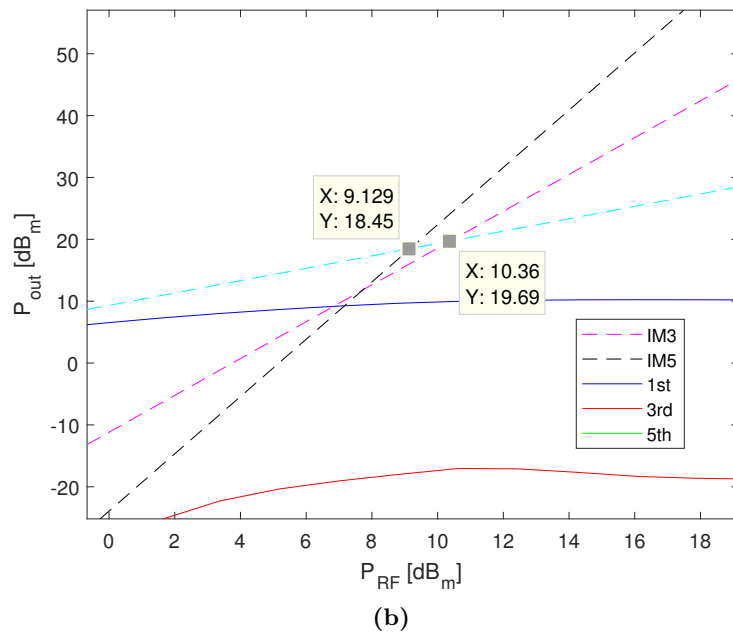
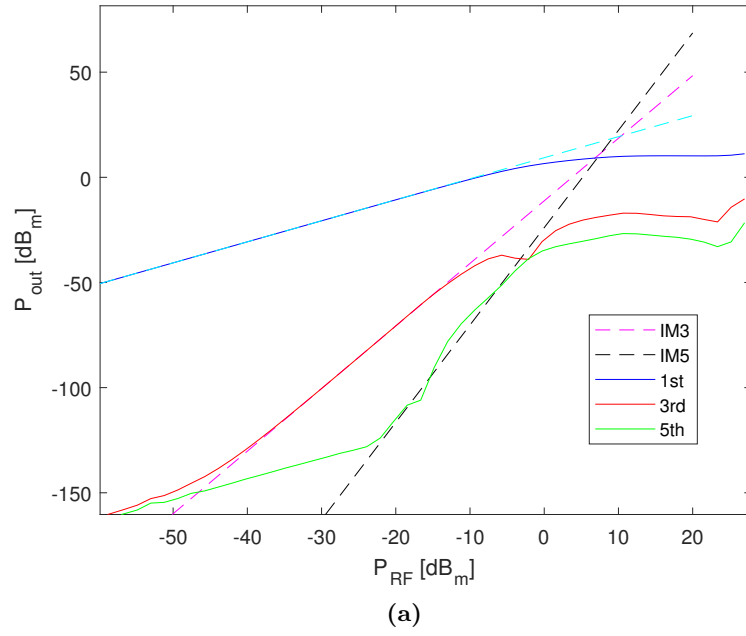


**Figure 40:** IIP<sub>3</sub> and IIP<sub>5</sub> in layout, one tone analysis.

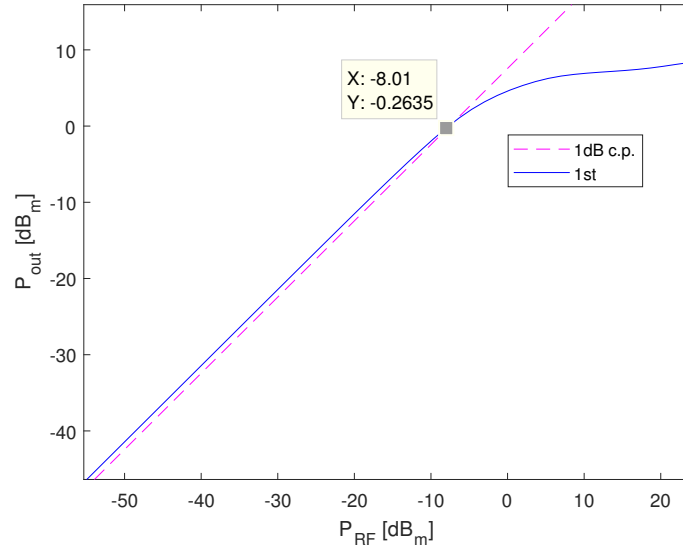
## 6.7 Two tone $IM_3$ and $CIM_3$ ratio

In order to simulate the behaviour of a non-monochrome, fixed-bandwidth signal, the two tone analysis has been carried on. Two RF tones at  $f_{RF}=110MHz$  and  $f_{RF}'=f_{RF}+\delta f=111MHz$  have been adopted. Figure 41 shows the 1dB compression point in this case. Third order intermodulation frequency components result to be at  $9MHz$  and  $12MHz$ . Their behaviour along with increasing input power is shown in figure 42a and 42b. Graphs show that power related to fundamental is strongly reduced when two tones are injected, since power is spread among all intermodulation products. Being the power moved from the fundamental to IMPs, input and output intercepts point result lowered with respect the 1-tone case.

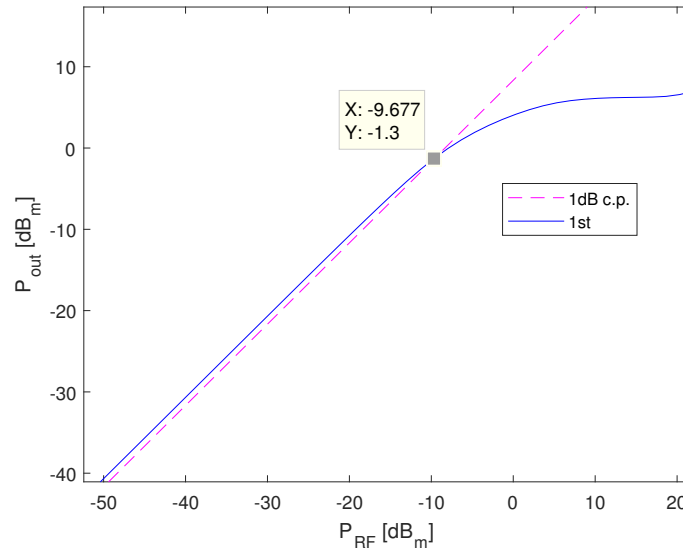
Frequency spectra at difference input power are shown in figure 43 and 44. From the latter, informations about the carrier and third intermodulation data are selected. In particular, the 1dB compression point spectrum has been chosen ( $P_{RF}=-9.68dB_m$ ), since this is set as the maximum input power accepted by the multiplier without heavy distortion. As it appears, power carried from fundamental tones (10MHz and 11MHz) barely increases after this point, whereas other tones keep increasing. Overall, the layout looks less performing as expected.

**Table 6:** 1dB compression point, IIP3 and CIM3 in two tones analysis.

| Parameter Name | Schematic | Layout | unit   |
|----------------|-----------|--------|--------|
| $P_{RF,1dB}$   | -8.01     | -9.68  | $dB_m$ |
| $IIP_3$        | 8.42      | 5.06   | $dB_m$ |
| $OIP_3$        | 16.9      | 14.4   | $dB_m$ |
| $CIM_{3,1dB}$  | 16.7      | 14.1   | dB     |

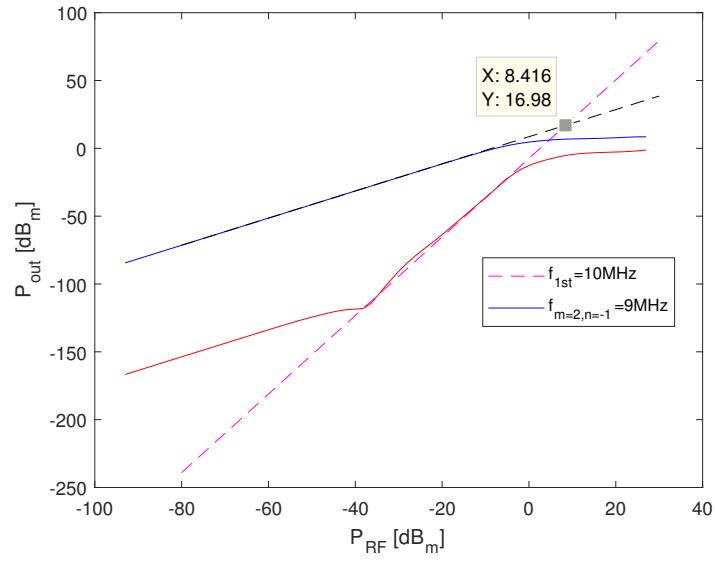


(a) *schematic*

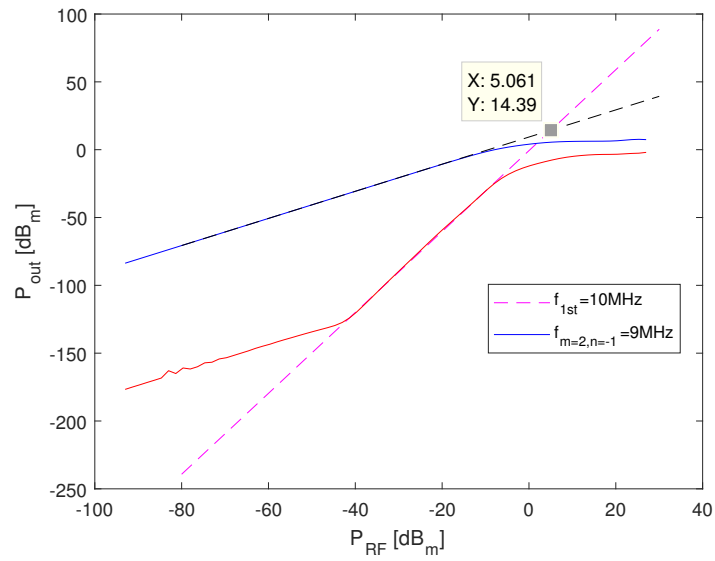


(b) *layout*

**Figure 41:** 1dB compression point, two tones.

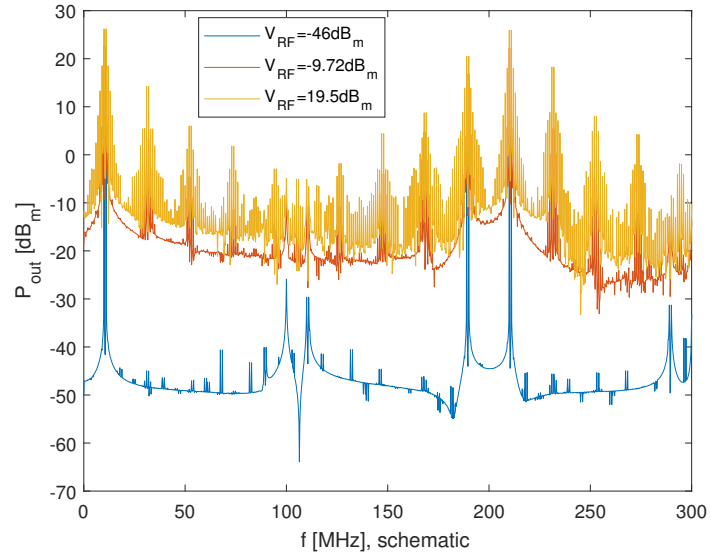


(a) *schematic*

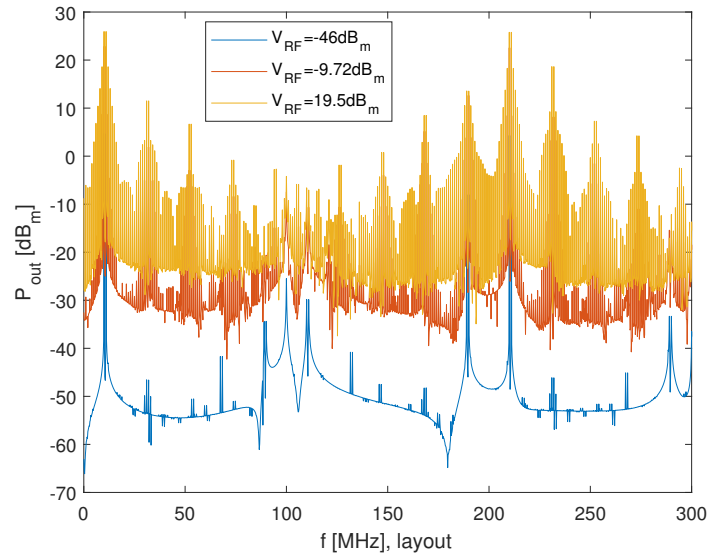


(b) *layout*

**Figure 42:** Harmonics power,  $IIP_3$  and  $IIP_5$  in schematic, two tone analysis.

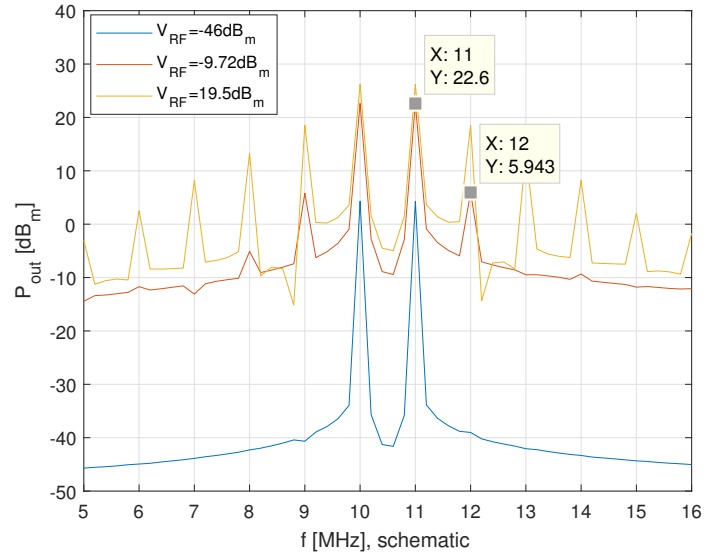


(a) *schematic*

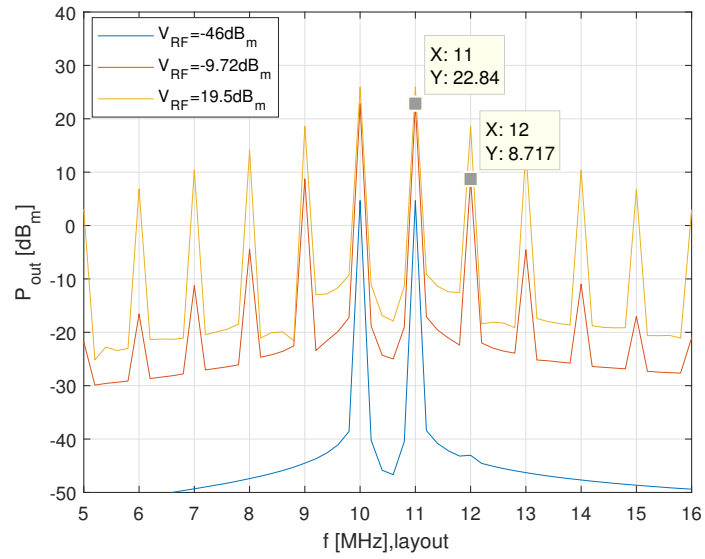


(b) *layout*

**Figure 43:** DFT, comparison between layout and schematic; cosine2 smoothing function.



(a) *schematic*



(b) *layout*

**Figure 44:** DFT, comparison between layout and schematic. CIM<sub>3</sub> measurement at 1dB compression point; cosine2 smoothing function.

## 7 Conclusions

The aim of this treatise was to show how to design a Gilbert cell based analog multiplier. A complete description of the GC working principle and a possible design procedure has been developed. Analysing the results obtained during the process, it is possible to notice that:

- The circuit correctly performs the mixing of an input signal within bandwidth;
- A reasonable conversion gain has been obtained ( $A_{v,layout} \simeq 2.9$ ,  $A_{v,schem} \simeq 2.7$ ), having a good matching between simulations and hand calculations;
- The amount of distortion introduced by the net is acceptable if the input power remains well below the 1dB compression point, limiting the circuit input range to a few hundreds of millivolts though;

However, despite these encouraging outcomes we need to point out that:

- The AMI's 0.6 process design kit by MOSIS is old-fashioned and not meant to be used for RF applications. Hence, the multiplier could not work correctly at the chosen frequency with the expected performances;
- The extractor used to generate the layout (Cadence Diva) was not able to provide the full set of parasitic elements that would appear within the circuit due to connections between components (routing, packaging) and originated by the devices themselves, leading to inaccurate analysis;
- A quite wide circuit area would be necessary in order to fulfil the specifications (gain, power consumption), determining the presence of large amount of parasitic elements that would worsen the circuit's performances in a real layout.

To sum up, the circuit functions properly, although it probably overestimates what would be the real behaviour. Thus we can say, with a certain amount of confidence, that all results and circuit performances shown here, would be by far worse if implemented on a physical device. Therefore, the design has to be intended with didactic purposes.

It was a great way for experimenting integrated analog design along with the use of professional cad tools. We learnt the importance of complex simulated device models in order to have functioning circuits in sub-micrometer technologies. It has been an opportunity to prove layout strategies dealing with MOSIS' integrated design rules.





## References

- [1] M. O. Bekkaoui. Gilbert cell mixer design in 65nm cmos technology. In *2017 4th International Conference on Electrical and Electronic Engineering (ICEEE)*, pages 67–72, 04 2017.
- [2] Arnold G Ruhumbika and Raed Abdulla. Analytical method for gain analysis of a double balanced gilbert cell mixer, 03 2014.
- [3] Steve Long. Presentation on rfc mas gilbert cell mixer design. <http://cp.literature.agilent.com/litweb/pdf/5989-9103EN.pdf>, 2001.
- [4] Gurukartheek Pedapalli. Design and characterization of cmos gilbert mixer at 130 nm technology for impedance measurement system of human cell in institute for nanoelectronics, 08 2014.
- [5] B. Razavi. *RF Microelectronics*. Prentice Hall communications engineering and emerging technologies series. Prentice Hall, 1998.
- [6] B. Razavi. *Design of Analog CMOS Integrated Circuits*. 2016.
- [7] G. O. B. Wolf, F. H. Gregorio, and J. E. Cousseau. Low noise design of a cmos gilbert mixer cell in 700 mhz. In *2015 XVI Workshop on Information Processing and Control (RPIC)*, pages 1–5, Oct 2015.